

Design, Synthesis, and Biological Evaluation of the Third Generation 17-Cyclopropylmethyl-3,14-dihydroxy-4,5-epoxy-6-[(4-pyridyl)carboxamido]morphinan (NAP) Derivatives as Mu/Kappa Opioid Receptor Dual Selective Ligands

Yi Zheng, Samuel Obeng, Huiqun Wang, Abdulmajeed M Jali, Bharath Peddibhotla, Dwight Williams, Chuanchun Zou, David L Stevens, William L Dewey, Hamid I Akbarali, Dana E Selley, and Yan Zhang
J. Med. Chem., **Just Accepted Manuscript** • DOI: 10.1021/acs.jmedchem.8b01158 • Publication Date (Web): 04 Jan 2019

Downloaded from <http://pubs.acs.org> on January 4, 2019

Just Accepted

“Just Accepted” manuscripts have been peer-reviewed and accepted for publication. They are posted online prior to technical editing, formatting for publication and author proofing. The American Chemical Society provides “Just Accepted” as a service to the research community to expedite the dissemination of scientific material as soon as possible after acceptance. “Just Accepted” manuscripts appear in full in PDF format accompanied by an HTML abstract. “Just Accepted” manuscripts have been fully peer reviewed, but should not be considered the official version of record. They are citable by the Digital Object Identifier (DOI®). “Just Accepted” is an optional service offered to authors. Therefore, the “Just Accepted” Web site may not include all articles that will be published in the journal. After a manuscript is technically edited and formatted, it will be removed from the “Just Accepted” Web site and published as an ASAP article. Note that technical editing may introduce minor changes to the manuscript text and/or graphics which could affect content, and all legal disclaimers and ethical guidelines that apply to the journal pertain. ACS cannot be held responsible for errors or consequences arising from the use of information contained in these “Just Accepted” manuscripts.

1
2
3 **Design, Synthesis, and Biological Evaluation of the Third Generation 17-**
4 **Cyclopropylmethyl-3,14 β -dihydroxy-4,5 α -epoxy-6 β -[(4'-**
5 **pyridyl)carboxamido]morphinan (NAP) Derivatives as Mu/Kappa Opioid**
6 **Receptor Dual Selective Ligands**
7
8
9
10
11
12
13
14
15

16 Yi Zheng^a, Samuel Obeng^a, Huiqun Wang^a, Abdulmajeed M. Jali^b, Bharath Peddibhotla^a,
17 Dwight A. Williams^a, Chuanchun Zou^a, David L. Stevens^b, William L. Dewey^b, Hamid I.
18 Akbarali^b, Dana E. Selley^b, Yan Zhang^{a*}
19
20
21
22
23
24
25
26
27

28 ^aDepartment of Medicinal Chemistry, Virginia Commonwealth University, 800 E. Leigh Street,
29 Richmond, Virginia 23298, United States
30
31

32 ^b Department of Pharmacology and Toxicology, Virginia Commonwealth University, 1112
33 East Clay Street, Richmond, Virginia 23298, United States
34
35
36
37
38
39
40
41
42
43
44
45
46
47
48
49
50
51
52
53
54
55
56
57
58
59
60

Abstract

Mu opioid receptor (MOR) agonists have been widely applied for treating moderate to severe pain. However, numerous adverse effects have been associated with their application, including opioid-induced constipation (OIC), respiratory depression, and addiction. Based on previous work in our laboratory, NAP, a 6 β -N-4'-pyridyl substituted naltrexamine derivative, was identified as a peripheral MOR antagonist that may be used to treat OIC. To further explore its structure activity relationship, a new series of NAP derivatives were designed, synthesized, and biologically evaluated. Among these derivatives, NFP and NYP significantly antagonized the antinociception effect of morphine. Whereas NAP acted mainly peripherally, its derivatives NFP and NYP actually can act centrally. Furthermore, NFP produced significantly lesser withdrawal symptoms than naloxone at similar doses. These results suggest that NFP has the potential to be a lead compound to treat opioid abuse and addiction.

Keywords: opioid receptor, antagonist, opioid addiction, withdrawal symptoms, dual-selectivity.

Introduction

Opioid receptors belong to the Class A rhodopsin-like G-protein coupled receptor (GPCR) family and may be classified into three main subtypes known as the μ opioid receptor (MOR), κ opioid receptor (KOR), δ opioid receptor (DOR).¹⁻⁴ Among them, MOR is the main pharmacological target for opioid medications, such as morphine.⁵ After agonist binding, the conformation change of the MOR will lead to activation of the receptor, which may further result in opening of inwardly rectifying K^+ (GIRK) channels, inhibition of the voltage-gated Ca^{2+} (VGCC) channels, and inhibition of adenylyl cyclase activity.⁶⁻⁹ These changes may further induce a variety of changes in membrane morphology, neurons excitation, neurotransmitters release, and expression of genes through the second messenger systems.¹⁰ The behavioral effects of MOR activation include antinociception and addiction or abuse.^{11, 12} Opioid addiction or abuse has become a global epidemic.^{13, 14} Moreover, opioid abuse increases the prevalence of diseases such as HIV, tuberculosis, and hepatitis, especially for users who inject these drugs.¹⁵⁻¹⁹ It is reported that over 33,000 people died due to opioid overdose in the US in 2015,²⁰ which has increased over 14 times in the last 20 years.²¹

Currently, there are two approaches to treat opioid addiction, which are detoxification and maintenance therapy by using opioid receptor agonists²²⁻²⁴, partial agonists²⁵⁻²⁷, or antagonists.^{28, 29} Among them, opioid antagonists have been used as potential opioid addiction treatments for years.^{28, 29} The synthesized opioid antagonists include peptide opioids and non-peptide opioids. CTOP (**Figure 1**) and CTAP (**Figure 1**) are cyclic peptides which are highly effective opioid antagonists with high MOR selectivity and metabolic stability, but their poor bioavailability limited their development as clinical therapeutics.³⁰⁻³² Compared to peptide opioids, non-peptide opioid antagonists may have advantages of high bioavailability, easily crossing the blood-brain barrier (BBB) and good metabolic stability.³² The classical opioid antagonists used in opioid addiction treatments are naltrexone (**Figure 1**) and naloxone (**Figure**

1
2
3 1). As a result of their different half-lives, naloxone is a short-acting medication while
4
5 naltrexone is used for long term treatment.^{33,34} As opioid antagonists, they don't carry the side
6
7 effects related to opioid agonists, such as addiction and respiratory suppression.³⁵ However,
8
9 high doses of naltrexone and naloxone may induce hepatotoxicity,^{36, 37} cardiovascular and
10
11 pulmonary problems.³⁸ Besides, the interactions between these compounds and the MOR or
12
13 KOR may induce mood changes^{39, 40} or block transmission of neurotransmitters⁴¹⁻⁴³, though
14
15 more evidences are still needed to further prove them.
16
17

18
19 The side effects associated with low selectivity MOR antagonists prompt researchers to
20
21 develop new opioid antagonists. β -funaltrexamine (β -FNA, **Figure 1**), a MOR antagonist, has
22
23 similar potency to the MOR and KOR.^{44b} Cyprodime (**Figure 1**), another MOR antagonist, has
24
25 moderate selectivity to the MOR ($K_{i, \delta/\mu} = 39$ and $K_{i, \kappa/\mu} = 10$).^{45, 46} Clocinnamox (**Figure 1**) and
26
27 methocinnamox (**Figure 1**) are potent MOR antagonists but with similar binding affinity to all
28
29 three opioid receptors.⁴⁷ Meanwhile, it has been reported that activation of the KOR and further
30
31 dynorphin release has a relationship with mood behaviors, such as drug-related withdrawal,
32
33 aversion and relapse induced by stress.⁴⁸ Studies have shown that norBNI ($K_{i, \kappa} = 1.8$ nM)
34
35 increased the symptoms of opioid withdrawal in rats, while in another study with KOR knock-
36
37 out mice precipitation of opioid withdrawal was not observed.^{49, 50a} De Marco et al studied a
38
39 new highly selective KOR partial agonist as anodyne with less harmful side effects.^{50b} These
40
41 studies suggest that KOR probably is a potential target for drug addiction and side effects
42
43 related to mood behaviors. Collectively, highly selective and potent opioid antagonists are still
44
45 extremely desirable.
46
47
48
49

50
51 Keeping this in mind, a number of new chemical entities have been designed and synthesized
52
53 by modifying the structure of naltrexone to achieve highly selective opioid ligands.⁵¹⁻⁵³ One
54
55 such compound from our lab, 17-cyclopropylmethyl-3,14 β -dihydroxy-4,5 α -epoxy-6 β -(4'-
56
57 pyridylcarboxamido)morphinan (NAP) (**Figure 1**), a 6 β -N-4'-pyridyl substituted naltrexamine
58
59
60

1
2
3 derivative was identified as a peripherally selective MOR antagonist ($K_{i, \delta/\mu} \approx 747$, $K_{i, \delta/\kappa} \approx 163$;
4 $ED_{50} = 0.0088$ mg/kg).⁵⁴⁻⁵⁶ To avoid diarrhea induced at high doses of NAP, the second
5
6 generation NAP derivatives were designed and synthesized by modifying the C(6)-pyridyl ring
7
8 system of NAP which was shown to interact with the MOR ‘address’ region. NMP, (17-
9
10 Cyclopropylmethyl-3,14 β -dihydroxy-4,5 α -epoxy-6 β -{[4’-(3’-
11
12 methylpyridyl)]carboxamido}morphinan), a second generation NAP derivative had improved
13
14 pharmacological properties compared to NAP since it not only acted as a peripherally selective
15
16 MOR antagonist but also improved motility of the gastrointestinal tract in vivo.^{57a, 58} Further
17
18 molecular modeling studies showed that the methyl group at 3’ position on the pyridyl group
19
20 could reinforce the interactions between NMP and the ‘address’ region of the MOR.⁵⁸ Based
21
22 on these previous study results, we sought to further explore the influence on binding affinity
23
24 of 3’ position on the pyridyl ring of NAP to opioid receptors based on the “message-address”
25
26 concept.^{57a, 58} Thus, we designed, synthesized, and biologically evaluated a series of new
27
28 compounds as the third generation NAP derivatives. Two new compounds, NFP and NYP,
29
30 were characterized in vitro and in vivo as opioid receptor antagonists. Interestingly, these two
31
32 compounds were found to be centrally acting with less withdrawal effects compared to
33
34 naloxone, which was contrary to the peripherally acting NAP and NMP.
35
36
37
38
39
40
41
42
43
44

45 **Results and Discussion**

46 **Molecular Design**

47
48
49 Our molecular modeling study on NAP in the three opioid receptors demonstrated that the
50
51 C(6)-pyridyl ring of NAP may strengthen the selectivity of NAP for the MOR over the DOR
52
53 and KOR through aromatic stacking and hydrogen-bonding interactions.⁴⁴ Meanwhile, a
54
55 molecular dynamics simulation study of NMP in the MOR, DOR and KOR showed that the 3’-
56
57 methyl group on the pyridyl ring may reinforce the π - π stacking interaction between the
58
59
60

aromatic pyridyl ring of NMP and W318^{7,35} of the MOR, which resulted in the high selectivity of NMP to the MOR over the DOR and KOR.⁵⁸ Further modeling study results indicated that the characteristics of the substituents on the 3' position of pyridyl ring of NAP derivatives, such as steric hindrance, electrostatic, and hydrophobic effects, may have significant effect on the binding affinity and selectivity of NAP derivatives to the three opioid receptors.⁵⁸ Therefore, in designing the third generation NAP derivatives, substitutions with different electronic, bulky, steric, and hydrophobic properties were introduced at the 3' position of pyridyl ring (**Figure 2**).

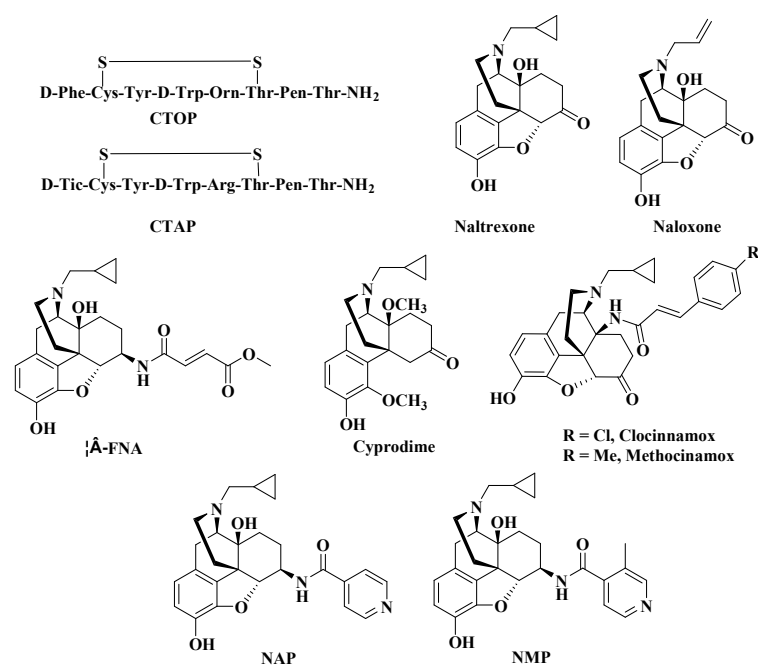


Figure 1. MOR selective antagonists.

Compounds	R	Compounds	R
1	F	7	C ₂ H ₅
2	CN	8	Isobutyl
3	NO ₂	9	Cyclopentyl
4	CF ₃	10	Cyclohexyl
5	COOH	11	Cycloheptyl

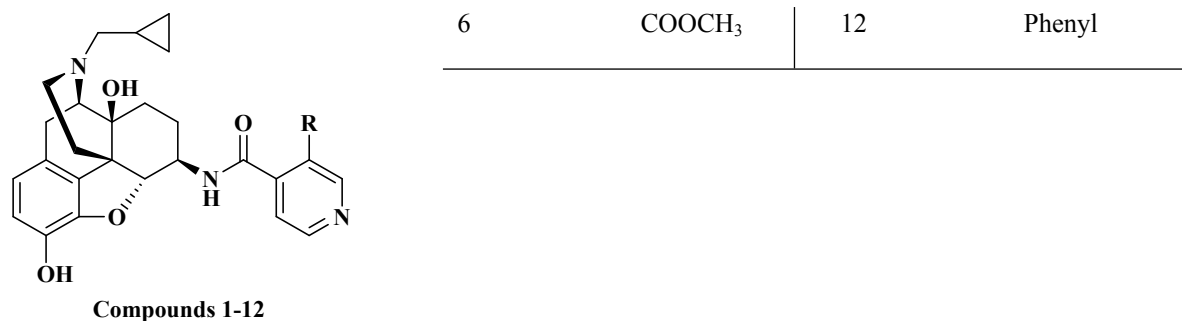
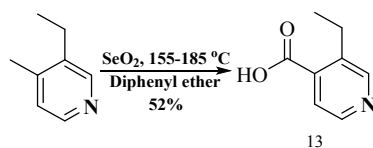
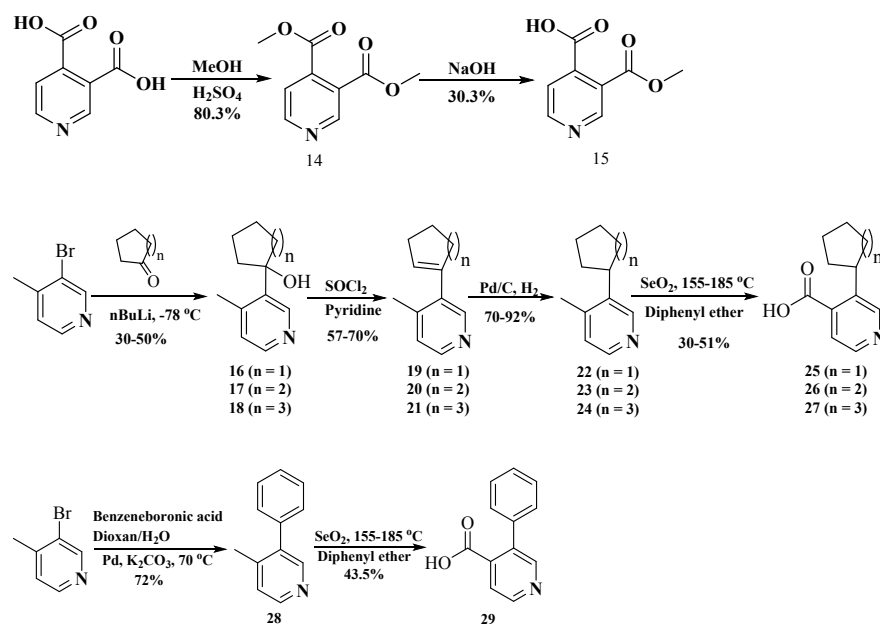


Figure 2. Structures of newly designed the third generation NAP derivatives.

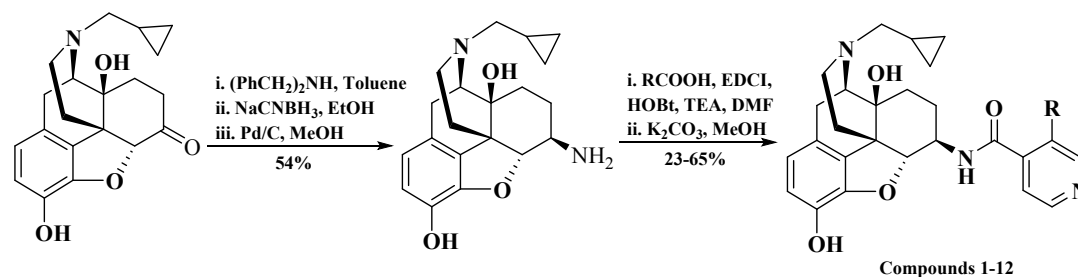
Chemistry

Twelve new NAP derivatives (**Table 1**) were synthesized. Compounds **1-6** were derivatives with electron-withdrawing groups at the 3' position on the pyridyl ring with a corresponding increment in size of the substituents. Compounds **7-12** were derivatives with electron-donating groups at the 3' position on the pyridyl ring with different bulkiness. For compounds **1-3**, **9** and **12**, the 3'-substituted pyridyl carboxylic acids were from commercial resources. For compounds **4-8**, **10** and **11**, the 3'-substituted pyridyl carboxylic acids had to be prepared by ourselves as shown in **Scheme 1** (Supporting information).^{57b,c,d} In addition, 6β-naltrexamine was synthesized as reported previously with a yield of 58% (**Scheme 2**).^{44a} Then, the 4'-pyridyl carboxylic acids were coupled with 6β-naltrexamine by EDCI/HOBt method.^{44, 57a} After that, the reaction crudes were treated with K₂CO₃ to get compounds **1-12** with reasonable yields (**Scheme 2**). All compounds were then transferred to hydrochloride salt and used for in vitro and in vivo studies.





24 Scheme 1. The synthesis of 3'-substituted pyridyl carboxylic acids for the newly designed NAP
25 derivatives.
26
27



Scheme 2. The synthesis route of the third generation NAP derivatives (compounds 1-12).

In vitro binding and functional studies were first conducted to evaluate the binding affinity, selectivity and efficacy of the compounds to the opioid receptors. In vivo studies were further conducted to characterize the behavioral profiles of these compounds.

In Vitro Radioligand Binding and MOR [³⁵S]GTP γ S Functional Studies

The competition radioligand binding assay was used to determine the binding affinity and selectivity of the new NAP derivatives for the MOR, KOR, and DOR. Chinese hamster ovary

(CHO) cell lines expressing mouse monocloned opioid receptors were used for this assay. The MOR was labeled with [³H]naloxone, while the KOR and DOR were both labeled with [³H]diprenorphine.

As shown in **Table 1**, all the compounds maintained subnanomolar binding affinity to the MOR except compounds **6** and **8** which showed nanomolar binding affinity. Compared to the first and second generation lead compounds, NAP ($K_{i, MOR} = 0.37 \pm 0.07$ nM) and NMP ($K_{i, MOR} = 0.58 \pm 0.25$ nM), most of the third generation derivatives still maintained high binding affinity to the MOR. This indicated that the substituent groups with different electronic properties and sizes at 3' position on the pyridyl ring did not significantly affect the binding affinity of these derivatives to the MOR. However, it is worth noting that esterification of the carboxylic acid at the 3' position (compound **6**) and introduction of an isobutyl group at the 3' position (compound **8**) resulted in a significant reduction in their MOR binding affinity. As mentioned above, the structural features of substituents on the 3' position of pyridyl ring, such as the steric hindrance, electrostatic, and hydrophobic effects, would significantly affect the binding affinity and selectivity of NAP derivatives to the three opioid receptors.⁵⁸ Compound **6** was an esterification product of compound **5**. After esterification, the original ionic interactions between carboxylic moiety in compound **5** and basic residues in the binding pocket of the MOR would be weakened in compound **6** significantly so that the binding affinity of compound **6** to the MOR was reduced. Furthermore, the isobutyl group on the pyridyl ring of compound **8** may result in steric clashes or unfavorable interactions with hydrophilic residues in the binding pocket that would decrease the binding affinity of compound **8** to the MOR. Interestingly, compared to compound **8**, compounds **9-12** carried even bulkier substituents on the pyridyl ring while still maintaining high binding affinities to the MOR at the subnanomolar level. One possible explanation of such an observation could be that the electrostatic and hydrophobic interactions induced by the much larger substituents on the pyridyl ring (compounds **9-11**) may

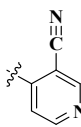
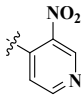
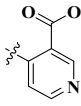
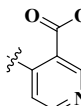
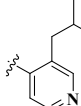
facilitate the compounds to interact with the binding pocket favorably in the MOR in a different binding mode than that of compound **8**.

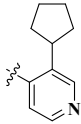
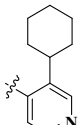
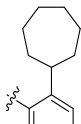
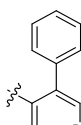
The selectivity of these compounds for the MOR over the DOR varied with different substituent groups at 3' position on the pyridyl ring. In general, derivatives with electron-withdrawing groups showed higher selectivity for the MOR over the DOR than derivatives with electron-donating groups. For example, compounds **1-6** showed more than 30-fold selectivity for the MOR over the DOR, especially for compounds **1** (NFP, $\delta/\mu = 435.8$) and **3** ($\delta/\mu = 562.4$). Both compounds had similar selectivity for the MOR over the DOR as NMP ($\delta/\mu = 470$). For the derivatives with electron-donating groups, compounds **7, 9, and 12** showed 50-134 fold selectivity for the MOR over the DOR while compounds **8, 10, and 11** showed 14-20 fold selectivity for the MOR over the DOR. Thus, it seemed that introduction of bulky and alkyl groups at position 3' on the pyridyl ring may reduce their selectivity for the MOR over the DOR.

On the KOR, there was a significant improvement in the binding affinity of all the compounds compared to NAP and NMP except for compound **8** which showed similar binding affinity to the KOR as of NAP and NMP. Compounds **1-7** and **9-12** maintained one-digit nanomolar or two-digit nanomolar binding affinity to the KOR. Thus, collectively, with substitution at 3' position on the pyridyl ring, the third generation NAP derivatives seemed to act as MOR/KOR dual-selective ligands.

Table 1. Radioligand binding results at the MOR, KOR, and DOR and [³⁵S]GTP γ S functional assay at the MOR for the third generation NAP derivatives.

Compounds	R	K _i (nM)			Selectivity		MOR [³⁵ S]GTP γ S Binding		
		MOR	DOR	KOR	δ/μ	κ/μ	EC ₅₀ (nM)	% E _{max}	of

									DAMGO
NTX ^a	N/A	0.26 ± 0.02	117.1 ± 8.9	5.15 ± 0.26	450	20	ND	7.75 ± 0.20	
NAP ^a		0.37 ± 0.07	277.5 ± 8.0	60.7 ± 5.6	747	163	1.14 ± 0.38	22.72 ± 0.84	
1(NFP)		0.36 ± 0.02	156.93 ± 7.81	4.80 ± 0.26	435.8	13.3	1.20 ± 0.19	34.97 ± 3.07	
2(NYP)		0.87 ± 0.09	46.29 ± 7.86	2.74 ± 0.47	53.2	3.1	1.28 ± 0.20	26.05 ± 0.74	
3		0.17 ± 0.02	95.61 ± 5.90	4.46 ± 0.11	562.4	26.5	0.53 ± 0.01	39.10 ± 2.57	
4		0.43 ± 0.01	61.79 ± 5.0	12.53 ± 0.89	143.7	29.1	1.38 ± 0.20	31.88 ± 3.39	
5		0.76 ± 0.08	55.58 ± 6.02	2.43 ± 0.19	73.2	3.2	1.83 ± 0.18	29.27 ± 1.42	
6		4.31 ± 0.29	137.31 ± 17.55	11.74 ± 1.15	31.9	2.7	13.40 ± 1.36	29.19 ± 0.84	
NMP ^b		0.58 ± 0.25	273.6 ± 1.8	96.7 ± 12.2	470	166	1.52 ± 0.26	30.63 ± 0.55	
7		0.32 ± 0.05	42.86 ± 8.27	9.18 ± 1.36	134.1	28.8	2.29 ± 0.28	41.65 ± 3.14	
8		7.20 ± 0.81	148.75 ± 15.96	75.63 ± 3.87	20.7	10.5	19.70 ± 2.37	27.30 ± 0.25	

9		0.60 ± 0.06	33.99 ± 3.99	8.16 ± 1.17	56.7	13.7	1.85 ± 0.16	56.67 ± 3.14
10		0.78 ± 0.09	11.24 ± 1.91	3.32 ± 0.54	14.4	4.2	2.46 ± 0.30	51.59 ± 3.73
11		0.93 ± 0.13	14.97 ± 2.44	5.16 ± 0.54	16.1	5.6	5.11 ± 0.16	48.32 ± 3.34
12		0.63 ± 0.05	44.83 ± 3.70	3.42 ± 0.38	71.1	5.4	1.46 ± 0.18	44.42 ± 3.12

^a reference 44a; ^b reference 57a

The [³⁵S]GTPγS functional assay was then conducted to determine the potency and relative efficacy of the synthesized compounds at the MOR. The potency was determined as the EC₅₀ while the efficacy was determined as the E_{max} relative to DAMGO, a MOR full agonist. From these results, it seemed that all the compounds acted as partial agonists with low to moderate efficacy. Derivatives with electron-withdrawing groups (compounds **1-6**) showed 20-40% MOR stimulation with one-digit nanomolar potency except compound **6**. Meanwhile, derivatives with electron-donating groups (compounds **7-12**) showed more than 40% efficacy with one or two-digit nanomolar potencies except compound **8** which had the lowest potency.

In Vivo Tail Immersion assay

All the newly synthesized NAP derivatives were further assessed for their acute agonistic and/or antagonistic effects using the tail immersion assay in mice as previously reported.^{44, 57}

1
2
3 The baseline latency (control) was determined before the tested compound was injected into
4 the mice. For the study of agonism, the time of tail immersion was 20 min (time that morphine's
5 antinociceptive effect starts to peak) after the test compound was injected (s.c.). For the study
6 of antagonism, the test compound was given 5 min before morphine. The tail immersion test
7 was then conducted 20 min after morphine was given. The percent maximum possible effects
8 (%MPE) was calculated for each mouse using at least five mice per drug. Briefly, the
9 derivatives were studied for their ability to produce antinociception or block the
10 antinociception produced by morphine (10 mg/kg). As shown in **Figure 3A**, none of these new
11 derivatives showed significant antinociception compared to morphine at the same dose (10
12 mg/kg). However, when they were tested as antagonists at the same dose (**Figure 3B**, 10
13 mg/kg), compounds **1** (NFP) and **2** (NYP) antagonized morphine's antinociception effect
14 significantly. The %MPEs of morphine (10 mg/kg) in the presence of NFP and NYP (10 mg/kg)
15 were only $6.2 \pm 2.4\%$ and $7.8 \pm 5.4\%$, respectively. The antagonism of NFP and NYP were
16 shown to be dose-dependent (**Figure 4A** and **4B**, AD_{50} values of NFP and NYP were 2.82
17 (1.34-5.94) mg/kg with 95% confidence level (CL) and 1.75 (0.88-3.47) mg/kg with 95% CL,
18 respectively). In contrast to NFP and NYP, other NAP derivatives did not significantly block
19 morphine's antinociception at the tested dose of 10 mg/kg. These results suggested that NFP
20 and NYP had the ability to cross the blood brain barrier (BBB) and block the analgesic effect
21 of morphine in CNS.

22
23
24
25
26
27
28
29
30
31
32
33
34
35
36
37
38
39
40
41
42
43
44
45
46
47 It was intriguing to us that two of the third generation NAP derivatives, NFP and NYP,
48 crossed the BBB and antagonized morphine's antinociception, while NAP was identified as a
49 P-glycoprotein substrate and failed to cross the BBB effectively. Apparently introduction of
50 fluoro and nitrile groups on the pyridyl ring may play an important role in improving their CNS
51 penetration. To be noted, about 5-15 % of drugs on the market are fluorinated compounds^{59, 60}
52 and it has been shown that these compounds have improved metabolic stability and
53
54
55
56
57
58
59
60

1
2
3 physicochemical properties. Meanwhile fluorination seems to enhance the CNS penetration
4 ability of non-CNS drugs and the efflux function of P-glycoprotein.^{61, 55} This may help explain
5 why NFP crossed the BBB while NAP did not.⁶¹ In addition, it has been reported that
6 introducing nitrile groups may also enhance metabolic stability and improve hydrogen bonding
7 interactions with residues in the orthosteric binding site of protein targets.⁶² Currently, there
8 are at least 30 drugs containing nitrile groups on the market and more than 20 drug candidates
9 containing nitrile groups under clinical trials.⁶² An example of such a drug is piritramide, an
10 opioid analgesic which crosses the BBB and is used for post-operation pain.⁶³

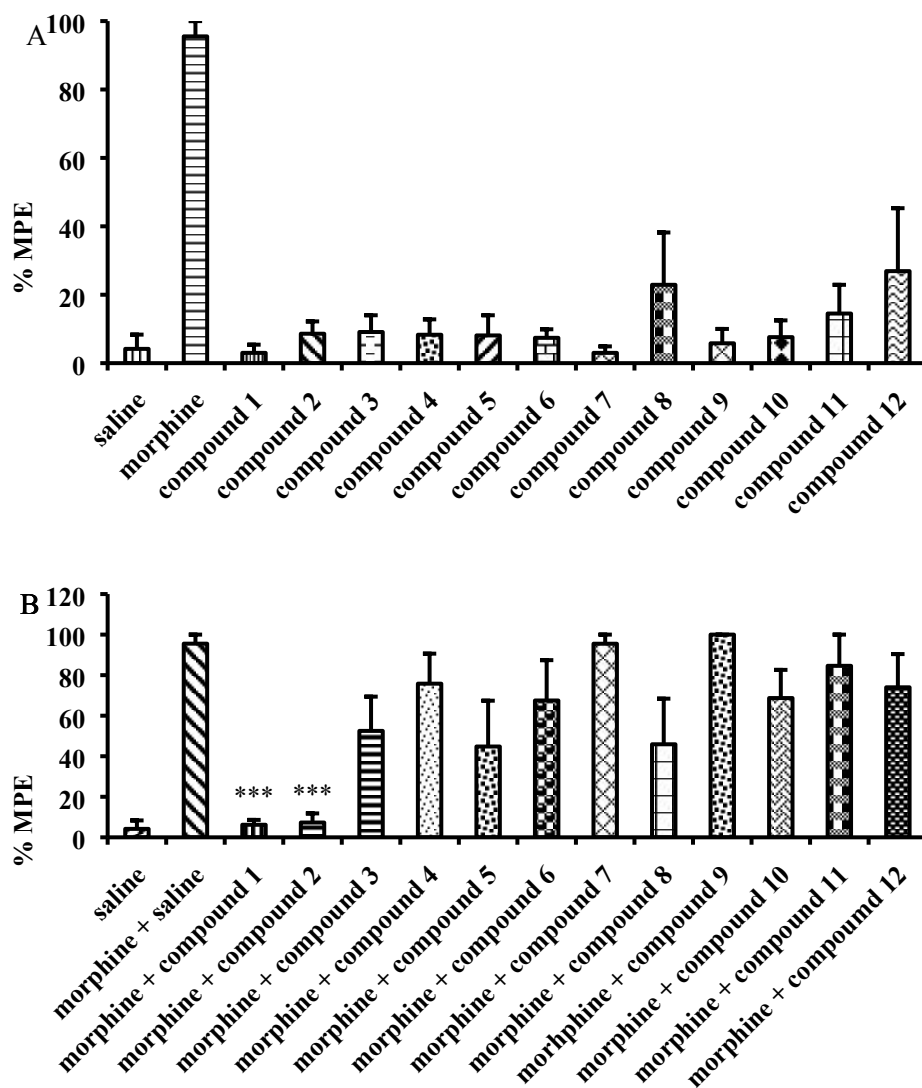


Figure 3. Tail immersion assay results for the third generation NAP derivatives as agonist (A) and antagonist (B) in the presence of morphine in mice at a single dose of 10 mg/kg. Morphine (10 mg/kg) and saline were used as positive and negative controls (n = 5, *** indicates P < 0.005).

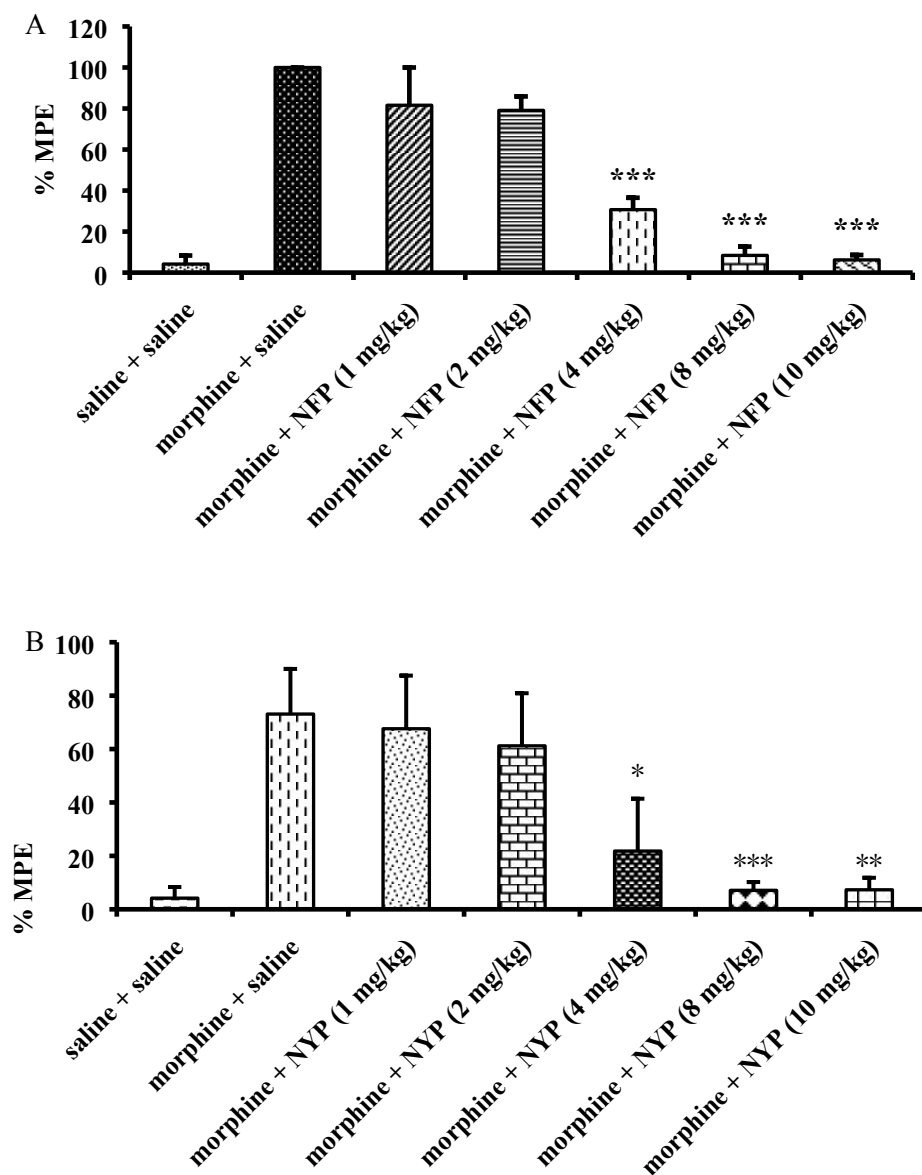
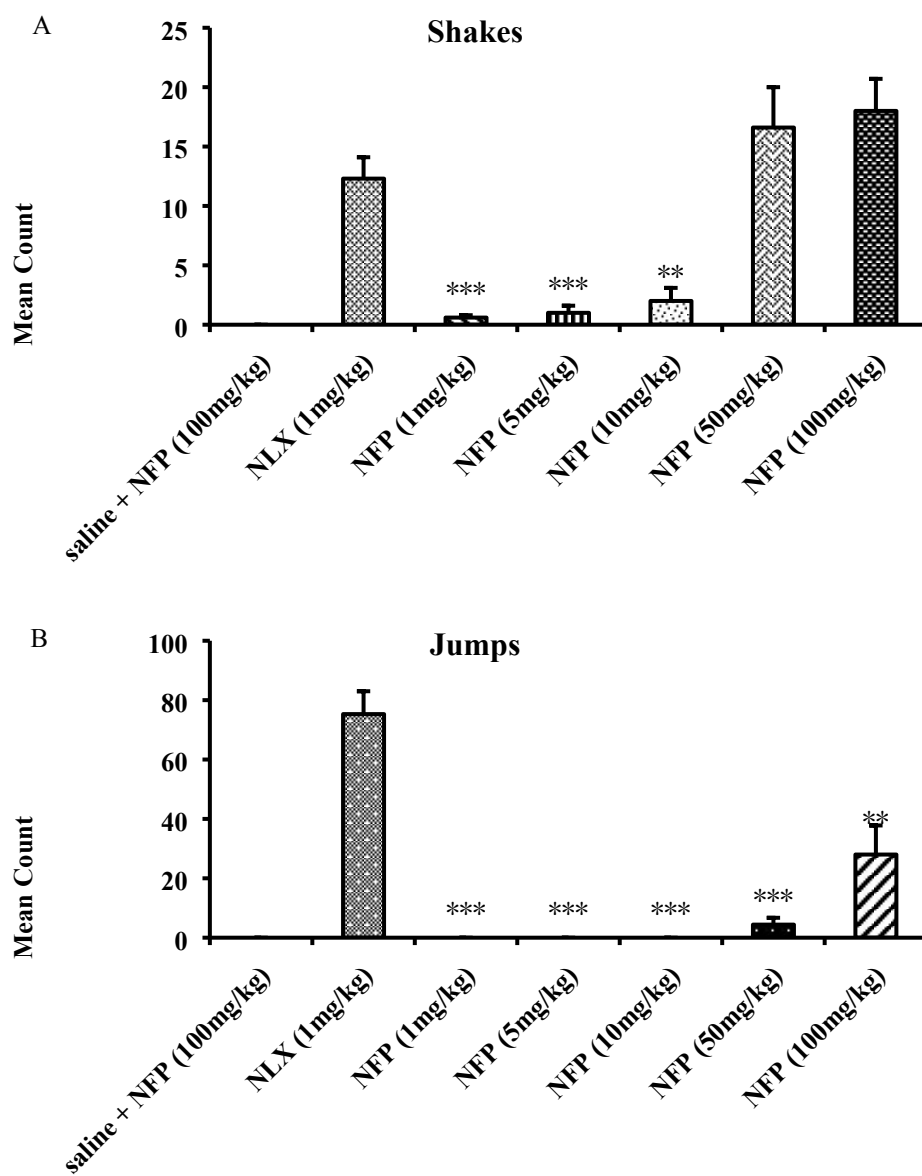


Figure 4. Dose-response studies of NFP (A) and NYP (B) as antagonists in mice. Morphine (10 mg/kg) and saline were used as positive and negative controls (n = 5, *** indicates P < 0.005).

In Vivo Withdrawal Study

Opioid antagonists such as naloxone and naltrexone have been applied to reverse the effects of opioid agonists in cases of opioid overdose and in opioid addiction treatments. However, it has been shown that naloxone and naltrexone produce significant withdrawal symptoms when administered, which limits their use in opioid addiction treatments.⁶⁴ Since NFP and NYP were identified as opioid antagonists in vivo, a withdrawal study was conducted using morphine-pelleted mice to determine whether these two compounds would produce withdrawal effects similar to naloxone. In this study, somatic symptoms of opioid withdrawal (shakes, jumps, and paw tremors) were quantified over a period of 20 minutes.^{55a} As shown in **Figure 5**, NFP produced significantly fewer wet dog shakes, jumps, and paw tremors at 10 mg/kg than naloxone at 1 mg/kg. Meanwhile, at much higher doses (50 and 100 mg/kg) NFP produced wet dog shakes (**Figure 5A**) and paw tremors (**Figure 5C**), but not significantly different from those of naloxone at 1 mg/kg. More interestingly, at a high dose of 50 mg/kg NFP still produced significantly fewer jumps (**Figure 5B**) than naloxone at 1 mg/kg. NYP, on the other hand, produced significantly fewer wet dog shakes and jumps at 1 mg/kg than naloxone at 1 mg/kg, but at doses 5 mg/kg and higher it produced wet dog shakes (**Figure 6A**) and jumps (**Figure 6B**) similar to naloxone at 1 mg/kg. Also, NYP produced similar paw tremors (**Figure 6C**) at 5 mg/kg similar to naloxone at 1 mg/kg.

It has been reported that naloxone can antagonize morphine's antinociception effect potently (AD_{50} at 3.1 mg/kg) in a tail flick assay^{55b} while it may induce significant withdraw symptom (e.g. Figures 5 and 6, at 1 mg/kg). Compared to naloxone, NFP can effectively across BBB entering into brain and reverse morphine's antinociception effect at a similar potency level but showed much lesser withdrawal symptoms. These results are very encouraging since they suggest that NFP may has potential application in opioid addiction treatments with more compatible patient compliance profiles compared to naloxone.



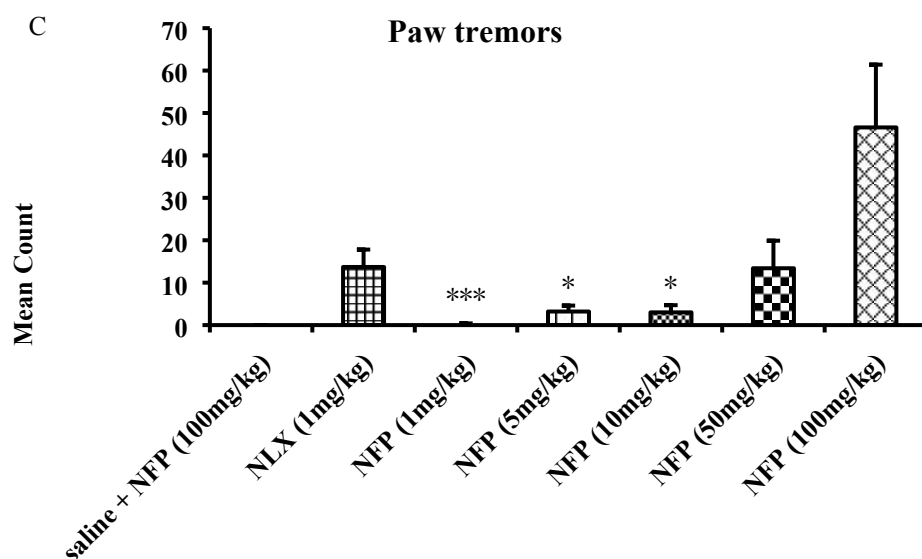
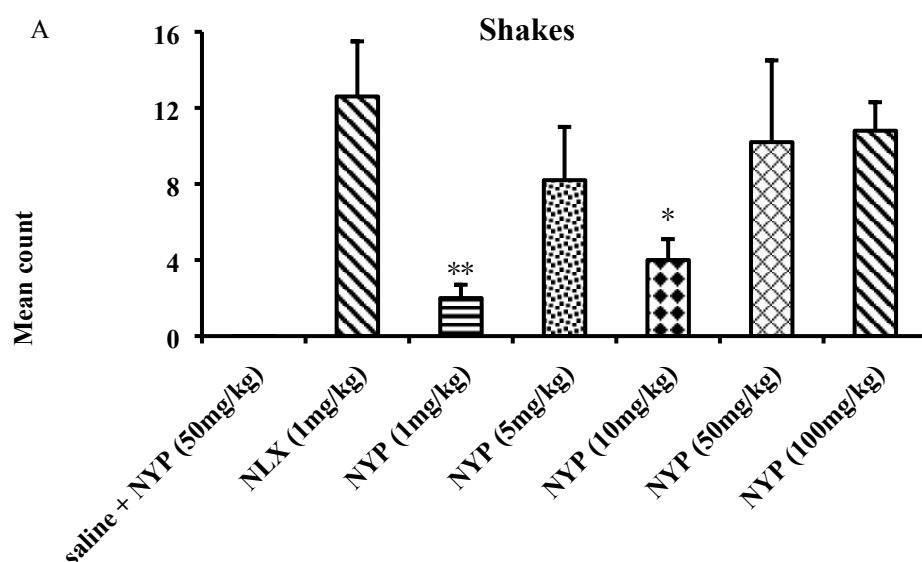


Figure 5. In vivo withdrawal study of NFP in morphine-pelleted mice (n=5). The first column in each figure represents the withdrawal effects of NFP in placebo-pelleted mice while the second to the seventh show the withdrawal effects of naloxone (NLX, 1mg/kg) and NYP in morphine-pelleted mice. (n = 5, * means $P < 0.05$, ** means $P < 0.005$, *** indicates $P < 0.0005$)



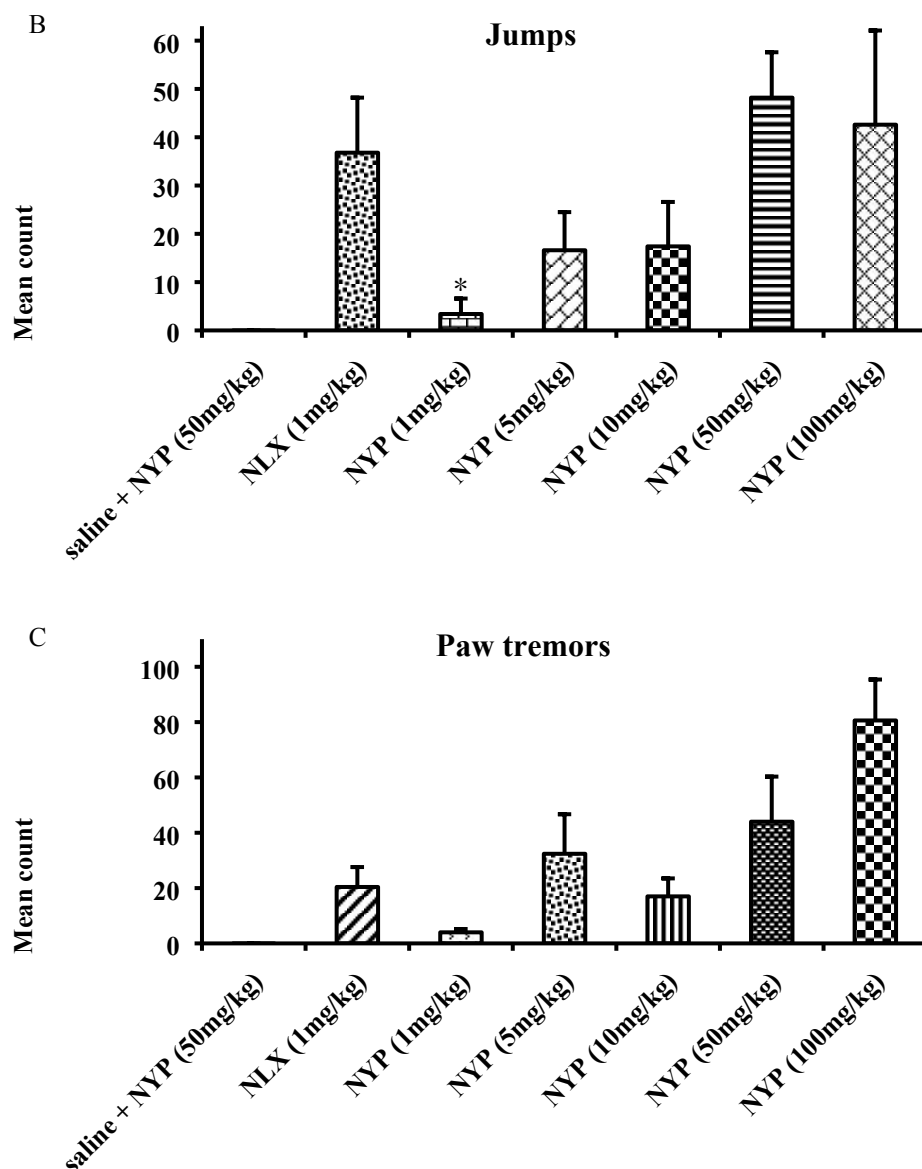


Figure 6. In vivo withdrawal study of NYP in morphine-pelleted mice ($n=5$). The first column in each figure represents the withdrawal effects of NYP in placebo-pelleted mice while the second to the seventh show the withdrawal effects of naloxone (NLX, 1mg/kg) and NYP in morphine-pelleted mice. ($n = 5$, * indicates $P < 0.05$, ** indicates $P < 0.005$, *** indicates $P < 0.0005$).

We then further characterized NFP's partial agonism and antagonism via concentration-effect curves for stimulation of $[^{35}\text{S}]\text{GTP}\gamma\text{S}$ binding in mMOR-CHO cells by NFP and DAMGO alone (Figure 7A) in comparison to NFP curves in the presence in an EC_{90} DAMGO concentration (Figure 7B). Naltrexone was examined as a positive control for MOR

antagonism (Figure 7B). Relative to DAMGO (normalized $E_{\max} = 100 \pm 2.6\%$ and $EC_{50} = 32.5 \pm 1.1$ nM), NFP was a partial agonist with an E_{\max} value of $34.9 \pm 1.5\%$ and EC_{50} value of 1.21 ± 0.19 nM, in agreement with our initial screening results (Table 1). In the presence of $0.3 \mu\text{M}$ DAMGO, NFP produced a concentration-dependent inhibition of DAMGO-stimulated $[^{35}\text{S}]\text{GTP}\gamma\text{S}$ binding, achieving maximal inhibition (minimum) at $37.7 \pm 1.5\%$ of the maximal stimulation produced by DAMGO. Similarly, naltrexone produced concentration-dependent inhibition, with maximal inhibition at $12.8 \pm 0.4\%$ of maxima DMAGO stimulation. Functional K_i values were then calculated from these data. NFP and naltrexone inhibited DAMGO-stimulated $[^{35}\text{S}]\text{GTP}\gamma\text{S}$ binding with K_i values of 0.86 ± 0.09 and 0.67 ± 0.05 nM, similar to their K_i values for MOR binding (Table 1). NFP had a relative efficacy that was approximately 35% of DAMGO and 3-fold that of naltrexone under these experimental conditions.

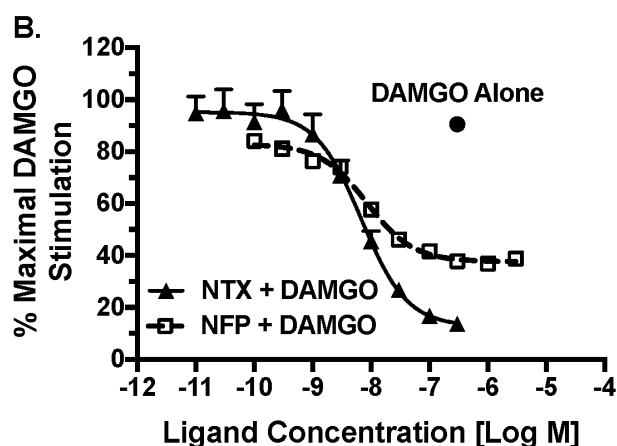
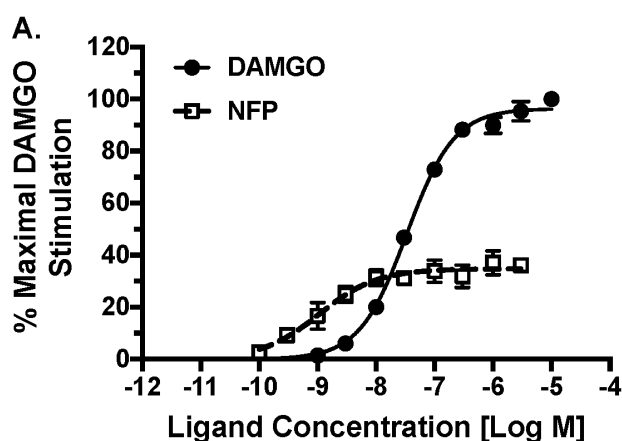


Figure 7. MOR partial agonism and antagonism by NFP in mMOR-CHO cells. Ligand concentration-effect for stimulation of [³⁵S]GTPγS binding in membranes from mMOR-CHO cells were determined alone (A) or in the presence of 0.3 μM DAMGO (B). Data are mean ± SEM (n = 4-5) of the percentage of maximal stimulation (produced by a maximally-effective DAMGO concentration of 0.3 μM).

Modeling study

As described above, NFP (**Figure 8**) showed dual-selective binding affinity to the MOR and KOR, and displayed significant selectivity over the DOR ($K_i, \delta/\mu = 435.8$). Meanwhile, NFP acted as an MOR partial agonist with moderate efficacy (Table 1) and a KOR partial agonist with low efficacy ($EC_{50} = 13.62 \pm 1.57$ nM, 26.71 ± 1.94 % max effect of U50,488H), and a DOR antagonist (EC_{50} not determined, 7.22 ± 1.17 % max effect of SNC80). However, the results of its in vivo studies displayed that NFP acted as an effective opioid antagonist in the CNS. To understand its selectivity profile to the opioid receptors, the antagonist-bound crystal structures of MOR (PDB ID: 4DKL)⁶⁴, KOR (PDB ID: 4DJH)⁶⁵ and DOR (PDB ID: 4EJ4)⁶⁶ were adopted from Protein Data Bank <http://www.rcsb.org> and NFP was docked into the three receptors by GOLD 5.4.^{67, 68} The binding poses of NFP with the highest CHEM-PLP scores from the docking studies were chosen as the optimal binding poses of the ligand in the MOR, KOR, and DOR.

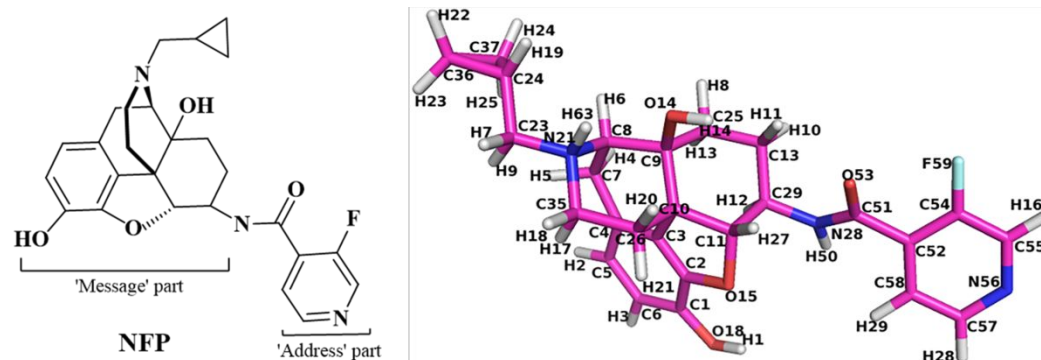


Figure 8. The chemical structure of NFP with atom notations from the docking studies.

1
2
3
4
5
6
7
8
9
10
11
12
13
14
15
16
17
18
19
20
21
22
23
24
25
26
27
28
29
30
31
32
33
34
35
36
37
38
39
40
41
42
43
44
45
46
47
48
49
50
51
52
53
54
55
56
57
58
59
60

Similar to the lead compound NAP, NFP was designed and synthesized according to the ‘message-address’ concept where the ‘message’ moiety (epoxymorphinan moiety) was assumed to determine its efficacy and the ‘address’ moiety (pyridyl ring) to contribute to its selectivity (**Figure 8**).⁵⁸ Comparing the binding poses of NFP in the MOR, KOR, and DOR with those of NAP, we found that the identical ‘message’ moiety of NFP and NAP bound with the same domain of the MOR, KOR, and DOR through similar interactions with the conserved residues in the three receptors.⁵⁸ Basically, the epoxymorphinan moiety formed hydrophobic interactions with the conserved residues M^{3.36}, W^{6.48} and H^{6.52} (superscript numbers follow the Ballesteros-Weinstein numbering method for GPCRs⁶⁹) and hydrogen bonding interactions with Y^{3.33}. Meanwhile, an ionic interaction was formed between the conserved D^{3.32} and the nitrogen atom at 17-position of the epoxymorphinan moiety of NFP (**Figure 9**). Collectively, the interactions between the ‘message’ moiety (epoxymorphinan moiety) of NFP and the conserved residues seemed to have no significant influence on the selectivity of NFP to the MOR, KOR, and DOR.

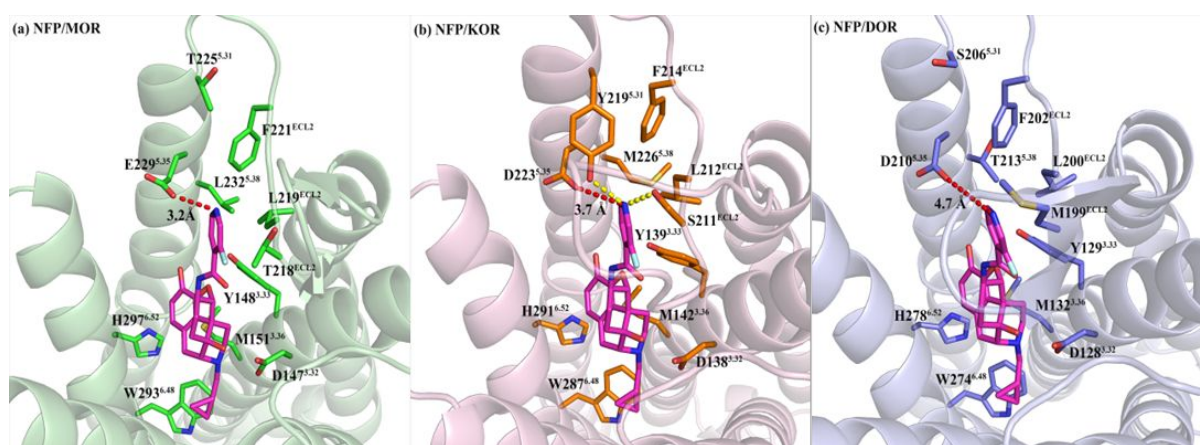


Figure 9. The docking studies results of NFP in the MOR (a, PDB ID: 4DKL), KOR (b, PDB ID: 4DJH), and DOR (c, PDB ID: 4EJ4), respectively, with the highest CHEM-PLP scores. NFP atoms: carbon (magenta); the key residue atoms in MOR: carbon (green); the key residue atoms in KOR: carbon (orange); the key residue atoms in DOR: carbon (light blue); oxygen

(red); nitrogen (blue). The red dashed lines represent the electrostatic interactions. The yellow dashed lines represent the hydrogen bonds.

The fluorine atom on the pyridyl ring ('address' moiety) of NFP is a strong electron withdrawing group which would weaken the capability of the nitrogen atom on the pyridyl ring of NFP to keep a proton compared to the case of NAP and NMP.⁵⁸ In consequence, the nitrogen atom on the pyridyl ring of NFP might form electrostatic interactions with the conserved residue E229^{5.35} in the MOR, D223^{5.35} in the KOR, and D210^{5.35} in the DOR. In addition, the pyridyl ring of NFP could also form hydrophobic interactions with the conserved hydrophobic residue L^{ECL2} and F^{ECL2} (**Table S1**). Thus, the 'address' moiety (pyridyl ring) of NFP seemed to bind to the same domain (termed 'address' domain) in the MOR, KOR, and DOR. However, several non-conserved residues located at this 'address' domain (T218^{ECL2}, T225^{5.31}, and L232^{5.38} in the MOR, S211^{ECL2}, Y219^{5.31}, and M226^{5.38} in the KOR and M199^{ECL2}, S206^{5.31}, and T213^{5.38} in the DOR, **Figure 9**) could also form direct interactions with the 'address' moiety (pyridyl ring) of NFP.

As the distances shown in **Figure 9**, the electrostatic interaction between the nitrogen atom on the pyridyl ring of NFP and E229^{5.35} in the MOR was much stronger than those in the NFP/KOR and NFP/DOR complexes, which may help to explain the highest affinity of NFP to the MOR. For the NFP/KOR complex, the non-conserved Y219^{5.31} and S211^{ECL2} could also form hydrogen bond with the nitrogen atom on the pyridyl ring of NFP, which may facilitate the binding of NFP to the KOR. However, for the NFP/DOR complex, no additional interaction being observed between the 'address' moiety of NFP and the residues located in the 'address' domain of DOR except the possibly weakest electrostatic one from D210^{5.35} (**Table S1**). Overall, the different interactions between the 'address' moiety of NFP and the 'address'

1
2
3 domain of the MOR, KOR, and DOR helped explain the binding affinity profile observed for
4
5 NFP in the three receptors.
6
7
8
9

10 **Conclusions**

11
12 Based on previous studies from our group, the third generation 6 β -N-4'-pyridyl substituted
13
14 naltrexamine derivatives were designed, synthesized and evaluated in both in vitro and in vivo
15
16 assays. The in vitro competition assays showed that the third generation compounds bearing
17
18 various substitutions at the 3' position of pyridyl ring carried a different selectivity profile than
19
20 NAP. In that, the third generation compounds were typically MOR/KOR dual-selective while
21
22 NAP was highly MOR selective. Most of the new compounds retained their binding affinity to
23
24 the MOR with subnanomolar level and one-digit nanomolar binding affinity to the KOR.
25
26 Meanwhile, most of the compounds had low to moderate efficacies at the MOR with one-digit
27
28 nanomolar potencies. Among these derivatives, NFP and NYP significantly antagonized the
29
30 antinociception produced by morphine in a dose dependent fashion. The in vivo studies showed
31
32 that NFP produced significantly lesser withdrawal symptoms than naloxone at similar doses.
33
34 These findings suggest that NFP may serve as a lead compound to develop novel MOR/KOR
35
36 dual selective ligand for treating opioid addiction and abuse.
37
38
39
40
41
42
43

44 **Experimental**

45 **Chemistry**

46 **General methods**

47
48 Reagents were purchased from either Sigma-Aldrich or Alfa Aesar. TLC analyses were
49
50 carried out on the Analtech Uniplate F254 plates. Chromatographic purification was conducted
51
52 on silica gel column (230-400 mesh, Merck). ¹H (400 MHz) and ¹³C (100 MHz) nuclear
53
54 magnetic resonance (NMR) spectra were recorded at ambient temperature with
55
56
57
58
59
60

1
2
3 tetramethylsilane as the internal standard on a Varian Mercury 400 MHz NMR spectrometer.
4
5 Melting points were recorded with OptiMelt Automated Melting Point System (Fisher
6
7 Scientific). IR spectra were obtained with Nicolet iS10 instrument (Thermo Scientific).
8
9 Applied Bio Systems 3200 Q trap with a turbo V source for TurbolonSpray was used for MS
10
11 analysis. HPLC analysis was performed by a Varian ProStar 210 system on Agilent Microsorb-
12
13 MV 100-5 C18 (250 mm × 4.6 mm) at 210 nm with water/acetonitrile (25/75, 30/70 or 35/65,
14
15 0.01% TFA in water) at 0.8 mL/min over 30 min. The purity of the third generation NAP
16
17 derivatives were determined by above analytical methods and their purity were identified as
18
19 $\geq 95\%$.
20
21
22
23
24
25

26 **General procedure**

27
28 N-(3-dimethylaminopropyl)-N'-ethylcarbodiimide hydrochloride (2.5 eq),
29
30 hydrobenzotriazole (2.5 eq), 4 Å molecular sieves, and trimethylamine (5 eq) were added to a
31
32 solution of the carboxylic acid (2.5 eq) in DMF on an ice-water bath under N₂ protection. After
33
34 30 min, a solution of 6β-naltrexamine (1 eq) in DMF was added dropwise. The mixture was
35
36 kept stirring overnight at room temperature and filtered the next day. The filtrate was then
37
38 concentrated under reduced pressure to remove the solvent. The residue was dissolved in
39
40 MeOH and potassium carbonate (2 eq) was added to the mixture. The reaction mixture was
41
42 stirred overnight at room temperature. Next day, the mixture was concentrated and the residue
43
44 was purified with silica gel column using methanol/dichloromethane (1% NH₃H₂O) as the
45
46 solvent system to obtain the target compounds.
47
48
49
50
51
52
53

54 **17-Cyclopropylmethyl-3,14β-dihydroxy-4,5α-epoxy-6β-[(3'-fluoro-4'-pyridyl)** 55 56 **acetamido]morphinan (compound 1, NFP)**

57
58 Compound **1** was synthesized as shown in the general procedure with a yield of 48%.
59
60

¹H NMR (400 MHz, CDCl₃) δ 8.94 (s, 1 H), 8.74 (d, *J* = 8.08 Hz, 1 H), 8.58 (m, 1 H), 8.43 (m, 1 H), 7.46 (t, *J* = 5.6 Hz, 1H), 6.51 (d, *J*=8.1 Hz, 1H), 6.45 (d, *J*=8.1 Hz, 1H), 4.77 (s, 1 H), 4.45 (d, *J*=8.1 Hz, 1 H), 3.52 (m, 1H), 2.90 (m, 2 H), 2.47 (m, 2 H), 2.21 (m, 2 H), 2.02 (m, 1 H), 1.87 (m, 1 H), 1.73 (m, 1 H), 1.48 (m, 1 H), 1.37 (m, 1 H), 1.21 (m, 1 H), 1.15 (m, 1 H), 0.73 (m, 1 H), 0.35 (m, 2 H), 0.01 (m, 2 H).

¹³C NMR (100 MHz, DMSO-*d*₆) δ 161.54, 156.46, 153.90, 146.23, 146.18, 142.06, 140.46, 139.10, 138.86, 131.24, 131.05, 130.93, 123.52, 123.23, 118.47, 117.12, 90.39, 69.52, 61.75, 58.38, 51.90, 47.06, 43.66, 30.32, 29.97, 24.33, 22.19, 9.22, 3.65, 3.52.

¹⁹F NMR (75 MHz, DMSO-*d*₆) δ -192.29.

IR (diamond, cm⁻¹) *V*_{max} 2942.19, 2829.33, 1655.64, 1529.02, 1487.78, 1454.25, 1416.41, 1322.93, 1238.29, 1204.29, 1186.88, 1152.58, 1131.78, 1100.14, 1034.82, 1017.27, 985.87, 942.11, 919.01, 898.28, 882.36, 799.14, 785.35, 763.19, 746.38, 667.00.

Mass Spectrum C₂₆H₂₈FN₃O₄ *m/z* calc. 465.2064 obs. 466.2159 [M + H]⁺. Mp 277.6-280.6 °C.

17-Cyclopropylmethyl-3,14β-dihydroxy-4,5α-epoxy-6β-[(3'-cyano-4'-pyridyl)acetamido]morphinan (compound 2, NYP)

Compound 2 was synthesized as shown in the general procedure with a yield of 48%.

¹H NMR (400 MHz, DMSO-*d*₆) δ 9.15-9.13 (m, 2 H), 8.94 (s, 1 H), 7.92 (d, *J* = 3.6 Hz, 1 H), 7.44 (s, 1 H), 7.31 (s, 1 H), 7.18 (s, 1 H), 6.77 (d, *J* = 8.08 Hz, 1 H), 6.69 (d, *J* = 8.08 Hz, 1 H), 5.06 (d, *J* = 8.24 Hz, 1 H), 3.38-3.33 (m, 3 H), 3.11-3.06 (m, 3 H), 2.9 (m, 1 H), 1.93-1.90 (m, 1 H), 1.51-1.43 (m, 3 H), 1.10-1.09 (m, 1 H), 0.67 (m, 1 H), 0.60 (m, 1 H), 0.51 (m, 1 H), 0.42 (m, 1 H).

¹³C NMR (100 MHz, DMSO-*d*₆) δ 167.45, 167.09, 156.63, 144.66, 142.37, 142.15, 139.45, 129.84, 125.95, 121.26, 120.30, 118.68, 117.50, 87.36, 70.14, 62.25, 57.32, 52.30, 47.03, 46.66, 30.59, 27.74, 23.65, 21.51, 6.32, 5.70, 3.24.

IR (diamond, cm^{-1}) V_{max} 3111.05, 2087.54, 1721.23, 1626.30, 1501.34, 1467.64, 1371.61, 1322.77, 1079.34, 1031.03, 858.34, 731.40.

Mass Spectrum $\text{C}_{27}\text{H}_{28}\text{N}_4\text{O}_4$ m/z calc. 472.2111 obs. 474.2049 $[\text{M} + 2\text{H}]^+$. Mp 222.8-224.5 °C.

17-Cyclopropylmethyl-3,14 β -dihydroxy-4,5 α -epoxy-6 β -(3'-nitro-4'-pyridyl)acetamido]morphinan (compound 3)

Compound **3** was synthesized as shown in the general procedure with a yield of 52%.

^1H NMR (400 MHz, $\text{DMSO}-d_6$) δ 9.16 (s, 1 H), 8.94 (m, 1 H), 8.87 (m, 1 H), 7.53 (m, 1 H), 6.50 (d, $J=8.1$ Hz, 1H), 6.44(d, $J=8.1$ Hz, 1H), 4.35(d, $J=7.8$ Hz, 1H), 3.42 (m, 1H), 2.90 (m, 2 H), 2.49 (m, 2 H), 2.22 (m, 2 H), 2.01 (m, 1 H), 1.88 (m, 1 H), 1.70 (m, 1 H), 1.57 (m, 1 H), 1.39 (m, 1 H), 1.19 (m, 2 H), 0.73 (m, 1 H), 0.35 (m, 2 H), 0.01 (m, 2 H).

^{13}C NMR (100 MHz, $\text{DMSO}-d_6$) δ 163.07, 154.58, 145.17, 142.56, 142.01, 140.49, 139.18, 131.16, 123.46, 122.82, 118.53, 117.14, 90.25, 69.52, 61.69, 58.32, 54.85, 52.11, 47.04, 43.66, 30.28, 29.84, 23.57, 22.18, 9.11, 3.68, 3.48.

IR (diamond, cm^{-1}) V_{max} 3072.08, 2952.94, 2820.03, 1681.02, 1639.45, 1615.13, 1567.61, 1550.22, 1531.35, 1451.63, 1393.77, 1357.98, 1348.34, 1329.88, 1277.14, 1262.58, 1253.30, 1241.33, 1227.99, 1189.63, 1147.14, 1121.29, 1035.17, 984.65, 945.33, 931.99, 922.82, 915.19, 896.65, 882.54, 858.32, 828.95, 806.17, 763.88, 740.60, 732.83, 721.00, 672.69.

Mass Spectrum $\text{C}_{26}\text{H}_{28}\text{N}_4\text{O}_4$ m/z calc. 492.2009 obs. 493.2087 $[\text{M} + \text{H}]^+$. Mp 266.46-269 °C.

17-Cyclopropylmethyl-3,14 β -dihydroxy-4,5 α -epoxy-6 β -(3'-trifluoromethyl-4'-pyridyl)acetamido]morphinan (compound 4)

Compound **4** was synthesized as shown in the general procedure with a yield of 51%.

^1H NMR (400 MHz, $\text{DMSO}-d_6$) δ 9.38 (s, 1 H), 9.04(s, 1 H), 9.02 (m, 1 H), 8.98 (m, 1 H), 7.56 (m, 1 H), 6.75 (d, $J=8.1$ Hz, 1H), 6.66 (d, $J=8.1$ Hz, 1H), 4.62(d, $J=8.1$ Hz, 1H), 3.38 (m, 1H),

3.04 (m, 2 H), 2.83 (m, 2 H), 2.43 (m, 2 H), 2.16 (m, 1 H), 1.82 (m, 2H), 1.84 (m, 1 H), 1.62 (m, 1 H), 1.41 (m, 1 H), 0.86 (m, 1 H), 0.76 (m, 2 H), 0.53 (m, 2 H).

^{13}C NMR (100 MHz, $\text{DMSO-}d_6$) δ 164.68, 154.10, 147.20, 143.25, 142.09, 141.39, 129.55, 123.01, 122.22, 121.83, 121.17, 119.33, 117.98, 89.34, 69.64, 61.60, 60.67, 51.54, 45.67, 32.18, 29.30, 27.69, 22.97, 21.96, 13.95, 5.71, 5.05.

^{19}F NMR (75 MHz, $\text{DMSO-}d_6$) δ -57.80.

IR(diamond, cm^{-1}) ν_{max} : 3216.30, 2935.48, 2831.91, 1676.72, 1607.94, 1557.26, 1502.39, 1471.37, 1452.47, 1422.76, 1377.05, 1328.16, 1281.32, 1194.14, 1132.27, 1081.31, 1054.16, 1038.57, 1027.12, 999.69, 982.16, 927.80, 890.56, 858.47, 821.56, 785.26, 720.13, 691.36, 675.16.

Mass Spectrum $\text{C}_{27}\text{H}_{28}\text{F}_3\text{N}_3\text{O}_4$ m/z calc. 515.2032 obs. 516.2089 $[\text{M} + \text{H}]^+$. Mp 224.9-227.5 °C.

17-Cyclopropylmethyl-3,14 β -dihydroxy-4,5 α -epoxy-6 β -(3'-carboxyl-4'-pyridyl)acetamido]morphinan (compound 5)

Compound **5** was synthesized as shown in the general procedure with a yield of 23%.

^1H NMR (400 MHz, $\text{DMSO-}d_6$) δ 9.14 (d, $J = 0.84$ Hz, 1 H), 9.12 (d, $J = 4.76$ Hz, 1 H), 8.99 (s, 1 H), 7.91 (d, $J = 1.08$ Hz, 1 H), 7.90 (d, $J = 0.92$ Hz, 1 H), 6.62-6.52 (m, 2 H), 4.99 (d, $J = 8.08$ Hz, 1 H), 4.92 (s, 1 H), 3.91-3.82 (m, 1 H), 3.16 (d, $J = 5.24$ Hz, 1 H), 3.03 (t, 2 H), 2.97 (s, 1 H), 2.63-2.60 (m, 1 H), 2.57-2.53 (m, 1 H), 2.40-2.30 (m, 2 H), 2.24-2.18 (m, 1 H), 2.02-1.95 (m, 1 H), 1.59-1.55 (m, 1 H), 1.18-1.44 (m, 1 H), 1.41-1.34 (m, 1 H), 1.26-1.23 (m, 1 H), 0.87-0.82 (m, 1 H), 0.48-0.46 (m, 2 H), 0.13-0.11 (m, 2 H).

^{13}C NMR (100 MHz, $\text{DMSO-}d_6$) δ 167.65, 167.25, 156.53, 144.44, 141.89, 141.13, 139.43, 125.90, 119.61, 117.53, 88.10, 70.04, 62.06, 58.80, 52.80, 49.03, 48.08, 44.14, 31.23, 22.66, 4.26, 4.00.

IR (diamond, cm^{-1}) V_{max} 3345.73, 3039.98, 2478.91, 2079.72, 1782.60, 1725.96, 1651.70, 1630.27, 1614.51, 1556.21, 1505.72, 1455.55, 1398.02, 1361.26, 1263.68, 728.87, 708.62

Mass Spectrum $\text{C}_{27}\text{H}_{29}\text{N}_3\text{O}_6$ m/z calc. 491.2056 obs. 474.2033 $[\text{M}-\text{CH}_3]^+$. Mp 271.2-273.7 °C.

17-Cyclopropylmethyl-3,14 β -dihydroxy-4,5 α -epoxy-6 β -[(3'-methyl formate-4'-pyridyl) acetamido]morphinan (compound 6)

Compound 6 was synthesized as shown in the general procedure with a yield of 32%.

^1H NMR (400 MHz, $\text{DMSO}-d_6$) δ 9.16 (s, 1 H), 9.12 (s, 1 H), 9.08 (s, 1 H), 9.00 (d, $J = 3.68$ Hz, 1 H), 7.91 (d, $J = 3.68$ Hz, 1 H), 7.76 (d, $J = 3.52$ Hz, 1 H), 7.31 (s, 1 H), 7.26 (d, $J = 8.24$ Hz, 1 H), 7.00 (d, $J = 8.24$ Hz, 1 H), 5.16 (7.26 (d, $J = 8.24$ Hz, 1 H)), 3.83 (s, 3H), 3.55 (s, 1 H), 3.50 (s, 1H), 3.36-3.35 (m, 1 H), 3.27-3.24 (s, 1 H), 3.23 (s, 2 H), 3.16-3.12 (m, 1 H), 2.95 (m, 1 H), 2.66-2.63 (m, 1 H), 1.99-1.95 (m, 1 H), 1.57-1.44 (m, 3 H), 1.23-1.19 (m, 1 H), 1.13 (m, 1 H), 0.69 (m, 1 H), 0.62 (m, 1 H), 0.54 (m, 1 H), 0.45 (m, 1 H).

^{13}C NMR (100 MHz, $\text{DMSO}-d_6$) δ 167.04, 165.51, 163.83, 156.57, 154.31, 150.66, 146.23, 144.61, 139.14, 134.01, 131.22, 130.14, 123.75, 122.67, 120.93, 117.47, 89.86, 70.03, 61.97, 57.38, 53.57, 52.41, 49.14, 46.62, 30.53, 27.58, 24.12, 21.11, 6.29, 5.70, 3.29.

IR (diamond, cm^{-1}) V_{max} 3554.62, 2953.39, 2088.05, 1716.47, 1633.27, 1557.57, 1489.97, 1446.28, 1367.76, 1290.11, 1263.40, 1234.61, 1193.08, 1152.84, 1128.11, 1101.15, 1076.56, 1032.71, 995.14, 960.71, 938.56, 914.77, 892.11, 855.03, 834.94, 797.66, 780.76, 732.58, 685.21, 662.07

Mass Spectrum m/z calc. $\text{C}_{28}\text{H}_{31}\text{N}_3\text{O}_6$ 505.2213 obs. 506.2227 $[\text{M} + \text{H}]^+$. Mp 210.5-212.3 °C.

17-Cyclopropylmethyl-3,14 β -dihydroxy-4,5 α -epoxy-6 β -[(3'-ethyl-4'-pyridyl) acetamido]morphinan (compound 7)

Compound 7 was synthesized as shown in the general procedure with a yield of 61%.

¹H NMR (400 MHz, DMSO-*d*₆) δ 9.00(s, 1 H), 8.50 (m, 2 H), 7.25 (m, 1 H), 6.70 (d, J=8.1 Hz, 1H), 6.54(d, J=8.1 Hz, 1H), 4.53(d, J=7.8 Hz, 1H), 3.61 (m, 1H), 3.01 (m, 2 H), 2.74 (q, J=7.6 Hz, 2H), 2.56 (m, 2 H), 2.29 (m, 2 H), 2.12 (m, 1H), 2.00 (m, 1H), 1.82 (m, 1 H), 1.62 (m, 1 H), 1.48 (m, 1 H), 1.34 (m,1 H), 1.25 (m, 1 H), 1.16(t, J=7.6 Hz, 3H), 0.84 (m, 1 H), 0.47 (m, 2 H), 0.12 (m, 2 H).

¹³C NMR (100 MHz, DMSO-*d*₆) δ 166.80, 150.49, 147.32, 143.38, 142.17, 140.54, 135.81, 131.33, 123.50, 120.89, 118.39, 117.10, 90.38, 69.58, 61.74, 58.37, 54.86, 51.53, 47.05, 43.68, 30.09, 24.32, 23.14, 22.19, 15.54, 9.22, 3.65, 3.51.

IR (diamond, cm⁻¹) V_{\max} 3307.45, 3084.08, 2946.81, 2931.57, 2822.35, 1659.73, 1592.75, 1530.90, 1503.18, 1471.36, 1454.36, 1431.17, 1404.97, 1368.65, 1322.47, 1260.16, 1239.39, 1227.39, 1190.27, 1154.54, 1128.18, 1114.19, 1096.93, 1082.03, 1059.66, 1036.40, 1028.24, 974.96, 932.47, 922.72, 915.97, 899.73, 877.40, 855.23, 818.18, 799.14, 784.30, 761.82, 744.37, 709.36, 675.07.

Mass Spectrum *m/z* calc. C₂₈H₃₃N₃O₄ 475.2471 obs. 476.2539 [M + H]⁺. Mp 238.6-241.3 °C.

17-Cyclopropylmethyl-3,14β-dihydroxy-4,5α-epoxy-6β-[(3'-isobutyl-4'-pyridyl)acetamido]morphinan (compound 8)

Compound **8** was synthesized as shown in the general procedure with a yield of 48%.

¹H NMR (400 MHz, CDCl₃) δ 8.61 (d, J = 5.04 Hz, 1 H), 8.58 (s, 1 H), 8.48-8.46 (m, 2 H), 7.86 (d, J = 5.04 Hz, 1H), 7.23 (d, J = 4.92 Hz, 1 H), 6.96 (d, J = 8.16 Hz, 1 H), 6.74 (d, J = 8.20, 1H), 4.56 (d, J = 4.80 Hz, 1 H), 4.27-4.21(m, 1H), 3.15 (s, 1 H), 3.11 (s, 1 H), 2.90-2.86 (m, 1 H), 2.68-2.66 (m, 2 H), 2.41-2.39 (m, 1 H), 2.27-2.25 (m, 1 H), 1.96-1.85 (m, 1 H), 1.65-1.63 (m, 1 H), 1.26 (s, 1 H), 0.93 (d, J = 2.20 Hz, 2 H), 0.91 (d, J = 2.16 Hz, 2 H), 0.84 (d, J = 7.96 Hz, 6 H), 0.57-0.55 (m, 2 H), 0.16-0.15 (m, 2H).

^{13}C NMR (100 MHz, CDCl_3) δ 167.37, 164.01, 153.50, 152.53, 148.14, 143.75, 137.28, 136.07, 134.23, 132.66, 132.14, 123.90, 122.76, 120.83, 119.34, 92.94, 69.91, 62.25, 59.63, 49.70, 47.07, 43.86, 40.21, 39.46, 30.39, 30.21, 28.70, 23.25, 22.55, 4.19, 3.94, 0.13..

IR (diamond, cm^{-1}) ν_{max} 3212.54, 3055.22, 2957.95, 2869.52, 2580.83, 2089.08, 1756.35, 1659.98, 1633.88, 1446.95, 1257.27, 1234.91, 1057.99, 851.95, 772.04, 666.71.

Mass Spectrum m/z calc. $\text{C}_{30}\text{H}_{37}\text{N}_3\text{O}_4$ 503.2784 obs. 504.2653 $[\text{M} + \text{H}]^+$. Mp 195.5-197.8 °C.

17-Cyclopropylmethyl-3,14 β -dihydroxy-4,5 α -epoxy-6 β -[(3'-cyclopentanyl-4'-pyridyl)acetamido]morphinan (compound 9)

Compound **9** was synthesized as shown in the general procedure with a yield of 58%.

^1H NMR (400 MHz, CDCl_3) δ 8.66(s, 1 H), 8.43 (m, 1 H), 7.05 (m, 1 H), 7.03 (m, 1H), 6.74 (d, $J=8.1$ Hz, 1H), 6.58(2 d, $J=8.1$ Hz, 1H), 4.45(d, $J=7.8$ Hz, 1H), 3.99 (m, 1H), 3.33 (m, 1 H), 3.06 (m, 2H), 2.63 (m, 2 H), 2.36 (m, 2 H), 2.18 (m, 2H), 2.08 (m, 2H), 1.83 (m, 3H), 1.65 (m, 16 H), 1.49 (m, 2 H), 0.82 (m, 1 H), 0.52 (m, 2 H), 0.12 (m, 2 H).

^{13}C NMR (100 MHz, $\text{MeOH-}d_4$) δ 170.58, 149.17, 147.62, 146.33, 143.88, 142.80, 140.26, 122.25, 120.57, 119.18, 92.20, 71.59, 64.10, 59.53, 53.32, 41.77, 35.59, 35.51, 31.29, 26.59, 25.02, 24.07, 5.35, 3.80.

IR (diamond, cm^{-1}) ν_{max} 3135.82, 3042.97, 2956.45, 2868.49, 1635.34, 1543.77, 1504.22, 1451.51, 1406.10, 1324.84, 1242.99, 1156.26, 1124.74, 1060.06, 1032.41, 1012.61, 986.31, 919.54, 855.36, 799.44, 781.28, 747.15, 677.37.

Mass Spectrum $\text{C}_{31}\text{H}_{37}\text{N}_3\text{O}_4$ m/z calc. 515.2784 obs. 516.2896 $[\text{M} + \text{H}]^+$. Mp 231.1-232.8 °C.

17-Cyclopropylmethyl-3,14 β -dihydroxy-4,5 α -epoxy-6 β -[(3'-cyclohexanyl-4'-pyridyl)acetamido]morphinan (compound 10)

Compound **10** was synthesized as shown in the general procedure with a yield of 51%.

¹H NMR (400 MHz, CDCl₃) δ 8.66(s, 1 H), 8.46 (m, 1 H), 7.11 (m, 1 H), 6.89 (m, 1H), 6.74 (d, J=8.1 Hz, 1H), 6.58(d, J=8.1 Hz, 1H), 4.43(d, J=7.8 Hz, 1H), 4.06 (m, 1H), 3.19 (m, 1 H), 2.91(m, 2H), 2.63 (m, 2 H), 2.36 (m, 2 H), 2.18 (m, 2H), 1.85 (m, 5H), 1.74 (m, 1 H), 1.66 (m, 2 H), 1.45 (m, 5H), 1.26 (m,3 H), 0.82 (m, 1 H), 0.52 (m, 2 H), 0.12 (m, 2 H).

¹³C NMR (100 MHz, MeOH-*d*₄) δ 172.30, 149.20, 147.66, 146.05, 143.84, 142.16, 141.31, 132.55, 125.43, 122.40, 120.11, 118.63, 92.74, 71.79, 63.78, 60.27, 53.44, 45.34, 40.59, 35.16, 34.94, 31.83, 31.36, 27.84, 27.73, 27.05, 25.56, 23.59, 10.25, 4.48, 4.20.

IR (diamond, cm⁻¹) *V*_{max} 3269.93, 2925.57, 2850.60, 1644.45, 1537.65, 1504.66, 1450.26, 1411.24, 1374.41, 1324.67, 1240.14, 1188.89, 1149.13, 1130.35, 1095.73, 1035.49, 984.59, 918.19, 881.92, 856.04, 828.64, 798.39, 785.52, 762.60, 745.35, 728.43, 702.73, 677.85.

Mass Spectrum C₃₂H₃₉N₃O₄ m/z calc. 529.2941 obs. 530.3025 [M + H]⁺. Mp 248.6-249.7 °C.

17-Cyclopropylmethyl-3,14β-dihydroxy-4,5α-epoxy-6β-[(3'-cyclohexanyl-4'-pyridyl)acetamido]morphinan (compound 11)

Compound **11** was synthesized as shown in the general procedure with a yield of 65%.

¹H NMR (400 MHz, CDCl₃) δ 8.58(s, 1 H), 8.43 (m, 1 H), 7.07 (m, 1 H), 6.89 (m, 1H), 6.74 (d, J=8.1 Hz, 1H), 6.58(d, J=8.1 Hz, 1H), 4.44 (d, J=7.8 Hz, 1H), 4.04 (m, 1H), 3.06(m, 3H), 2.63 (m, 2 H), 2.36 (m, 2 H), 2.18 (m, 2H), 1.47-1.92 (m, 17H), 0.83 (m, 1 H), 0.52 (m, 2 H), 0.13 (m, 2 H).

¹³C NMR (100 MHz, MeOH-*d*₄) δ 170.34, 149.43, 147.35, 145.13, 143.83, 143.39, 142.18, 132.54, 125.41, 122.28, 120.11, 118.62, 92.74, 71.79, 63.78, 60.27, 53.43, 45.35, 42.38, 37.53, 37.42, 31.82, 31.36, 28.74, 28.73, 28.63, 28.47, 25.64, 23.59, 10.23, 4.48, 4.19.

IR (diamond, cm⁻¹) *V*_{max} 3269.95, 3074.45, 2923.19, 2853.17, 1644.22, 1536.48, 1504.37, 1453.20, 1411.13, 1374.26, 1324.43, 1239.86, 1186.87, 1154.29, 1129.40, 1095.41, 1035.39, 984.37, 918.44, 896.79, 882.17, 856.61, 829.74, 798.64, 785.78, 762.42, 745.58, 728.45,

703.20, 676.77.

Mass Spectrum $C_{33}H_{41}N_3O_4$ m/z calc. 543.3097 obs. 544.3253 $[M + H]^+$. Mp 240.1-242.5 °C.

**17-Cyclopropylmethyl-3,14 β -dihydroxy-4,5 α -epoxy-6 β -(3'-Phenyl-4'-pyridyl)
acetamido]morphinan (compound 12)**

Compound **12** was synthesized as shown in the general procedure with a yield of 60%

1H NMR (400 MHz, DMSO- d_6) δ 9.06(s, 1 H), 8.66(s, 1 H), 8.65 (m, 2 H), 7.48 (m, 4 H), 7.37 (m, 2H), 6.60 (d, J=8.1 Hz, 1H), 6.51(d, J=8.1 Hz, 1H), 4.43(d, J=7.8 Hz, 1H), 3.48 (m, 1H), 3.17 (m, 1 H), 2.96 (m, 2H), 2.56 (m, 2 H), 2.30 (m, 2 H), 2.07 (m, 1H), 1.96 (m, 1H), 1.82 (m, 1 H), 1.54 (m, 1 H), 1.39 (m, 1 H), 1.23 (m,3 H), 0.83 (m, 1 H), 0.46 (m, 2 H), 0.11 (m, 2 H).

^{13}C NMR (100 MHz, DMSO- d_6) δ 166.73, 150.11, 148.48, 143.55, 142.12, 140.48, 136.30, 133.45, 131.25, 128.25, 128.49, 127.80, 123.45, 121.48, 118.56, 117.07, 90.18, 69.51, 61.69, 58.33, 51.59, 48.57, 46.95, 43.67, 29.87, 23.71, 22.16, 9.18, 3.66, 3.49.

IR (diamond, cm^{-1}) V_{max} 3267.19, 2926.62, 1759.45, 1655.72, 1537.27, 1490.98, 1477.79, 1445.55, 1399.94, 1329.53, 1277.45, 1236.21, 1200.83, 1154.28, 1131.52, 1095.64, 1068.52, 1037.44, 1006.16, 984.61, 934.19, 914.70, 880.93, 852.37, 793.70, 758.91, 699.07, 671.71.

Mass Spectrum $C_{32}H_{33}N_3O_4$ m/z calc. 523.2471 obs. 524.2552 $[M + H]^+$. Mp 232.4-235.2 °C.

Biological Evaluation

Drugs and Chemicals. Morphine (morphine sulfate pentahydrate salt) and naloxone, were procured from the National Institute of Drug Abuse (NIDA), Bethesda, MD and then made into a 10 μ M stock solution by dissolving in distilled water which was further diluted to the desired concentrations. All other reagents were purchased from either Sigma-Aldrich or Thermo Fisher.

1
2
3 **Animals.** Male Swiss Webster mice (25-30 g, 7-8 weeks, Harlan Laboratories, Indianapolis,
4 IN) were raised in animal care quarters and maintained at room temperature on light-dark cycle.
5
6 Food and water were available ad libitum. Protocols and procedures were approved by the
7
8 Institutional Animal Care and Use Committee (IACUC) at Virginia Commonwealth University
9
10 and complied with the recommendations of the IASP (International Association for the Study
11
12 of Pain).
13
14
15
16
17
18

19 **Competitive Radioligand Binding and [³⁵S]GTP γ S Functional Studies.**

20
21 In the competition binding assay, 30 μ g of membrane protein was incubated with the
22
23 corresponding radioligand in the presence of different concentrations of test compounds in
24
25 TME buffer (50 mM Tris, 3 mM MgCl₂, and 0.2 mM EGTA, pH 7.4). The bound radioligand
26
27 was separated by filtration using the Brandel harvester. Specific (i.e., opioid receptor-related)
28
29 binding at the MOR, KOR, and DOR was determined as the difference in binding obtained in
30
31 the absence and presence of 5 μ M naltrexone, U50,488, and SNC80, respectively. The IC₅₀
32
33 values were determined and converted to K_i values using the Cheng–Prusoff equation.
34
35
36

37
38 In the [³⁵S]GTP γ S functional assay, 10 μ g of MOR-CHO membrane protein was incubated
39
40 with 10 μ M GDP, 0.1 nM [³⁵S]GTP γ S, assay buffer (TME + 100 mM NaCl) and varying
41
42 concentrations of the compounds under investigation for 90 minutes in a 30 °C water bath.
43
44 Non-specific binding was determined with 20 μ M unlabeled GTP γ S. 3 μ M of DAMGO was
45
46 included in the assay as maximally effective concentration of a full agonist for the MOR. All
47
48 assays were determined in duplicate and repeated at least 4 times. Percent DAMGO-stimulated
49
50 [³⁵S]GTP γ S binding was defined as (net-stimulated binding by ligand/net-stimulated binding
51
52 by 3 μ M DAMGO) x 100%.
53
54
55
56
57
58
59
60

1
2
3 **Data Analysis of [³⁵S]GTPγS Binding Assays.** All samples were assayed in duplicate and
4 repeated at least four times for a total of ≥4 independent determinations. Results were reported
5 as mean values ± SEM. Concentration-effect curves were fit by nonlinear regression to a one-
6 site binding model, using GraphPad Prism software, to determine EC₅₀ and Emax values. IC₅₀
7 values were obtained from Hill plots, analyzed by linear regression using GraphPad Prism
8 software. Binding K_i values were determined from IC₅₀ values using the Cheng-Prusoff
9 equation: $K_i = IC_{50}/(1 + ([L]/K_D))$, where [L] is the concentration of competitor and K_D is the
10 K_D of the radioligand.
11
12
13
14
15
16
17
18
19
20
21
22
23

24 **Tail Immersion Test.** Swiss Webster mice (5 male mice for each group, 7-8 weeks, ENVIGO)
25 were used for this experiment. Water bath temperature was maintained at 56 ± 0.1 °C. The
26 baseline latency (control) was determined before the test compound was injected
27 subcutaneously (s.c.) into the mice. The average baseline latency obtained for this experiment
28 was 3.0 ± 0.1 s and only mice with a baseline latency of 2 to 4 s were used. For the agonism
29 study, tail immersion was conducted 20 min (time that morphine's antinociceptive effect starts
30 to peak) after the test compound was injected. To prevent tissue damage, a 10 s maximum cut
31 off time was imposed. Antinociception response was calculated as the percentage maximum
32 possible effect (%MPE), where $\%MPE = [(test - control) / (10 - control)] \times 100$. For the
33 antagonism study, the test compound was given 5 min before morphine. Tail immersion was
34 then conducted 20 min after giving morphine. %MPE was calculated for each mouse using at
35 least five mice per drug. AD₅₀ values were calculated using the least-squares linear regression
36 analysis followed by calculation of 95% confidence interval by Bliss method.
37
38
39
40
41
42
43
44
45
46
47
48
49
50
51
52
53
54
55

56 **Withdrawal Assay.** Swiss Webster mice (5 male mice for each group, 7-8 weeks, ENVIGO)
57 were used for the withdrawal study. A 75 mg morphine pellet was implanted into the base of
58
59
60

1
2
3 the neck of the mice and the mice were then given time to recover in their home cages. Before
4 the test began, 30 min was given to the mice for habituation to an open-topped, square, clear
5 Plexiglas observation chamber (26 x 26 x 26 cm³) with lines partitioning the bottom into
6 quadrants. All drugs and test compounds were administered by subcutaneous injection (s.c.).
7
8 The withdrawal was precipitated 72 h from pellet implantation with naloxone (1 mg/kg, s.c.),
9
10 and the test compounds at different doses. Withdrawal commenced within 3 min after
11 antagonist administration. Escape jumps, paw tremors, and wet dog shakes were quantified by
12 counting their occurrences over 20 min for each mouse (five mice per group). The data is shown
13 as the mean \pm SEM.
14
15
16
17
18
19
20
21
22
23
24
25

26 **Statistical Analysis.** One-way ANOVA followed by the posthoc Dunnett test were performed
27 to assess significance using Prism 6.0 software (GraphPad Software, San Diego, CA).
28
29
30
31
32

33 **Docking study**

34
35 The crystal structures of the MOR (PDB ID: 4DKL), KOR (PDB ID: 4DJH) and DOR (PDB
36 ID: 4EJ4) obtained from the Protein Data Bank at <http://www.rcsb.org>. Sybyl-X 2.0.⁵⁸ was
37 used to add hydrogen atoms to each receptor and to sketch NFP (TRIPOS Inc., St. Louis, MO).
38 NFP was then assigned Gasteiger-Hückel charges and energy minimized to a gradient of 0.05
39 under the TAFF in Sybyl-X 2.0.⁵⁸
40
41
42
43
44
45

46 GOLD 5.4 with default settings was used to conduct the docking study. The atoms within 10
47 Å of the γ -carbon atom of D^{3.32} of the MOR, KOR, and DOR were defined as the binding site
48 in the three receptors. Automated docking was conducted with a distance constraint of 4 Å
49 between the nitrogen atom at the 17' position of the epoxymorphinan skeleton and the
50 conserved D^{3.32}. In addition, a hydrogen bond constraint was applied between NFP's
51 dihydrofuran oxygen and the phenolic oxygen of the conserved Y^{3.33}. The highest scored
52
53
54
55
56
57
58
59
60

1
2
3 solutions (CHEM-PLP) were selected and merged into the receptor to obtain the optimal
4 binding poses of NFP in the MOR, KOR, and DOR. After docking, the binding poses were
5 energy minimized in Sybyl-X 2.0.7 with 5000 iterations under TAFF to remove the clashes
6 and strain energy between NFP and the three receptors.⁷⁰
7
8
9
10
11
12
13

14 **Author Information**

15 Yi Zheng: yzheng3@vcu.edu

16 Samuel Obeng: obengs@vcu.edu

17 Huiqun Wang: hwang6@vcu.edu

18 Dwight A. Williams: dwight.williams@kzoo.edu

19 David L. Stevens: david.stevens@vcuhealth.org

20 Chuanchun Zou: zigzaghk@126.com

21 Bharath Peddibhotla: peddibhotlab@vcu.edu

22 Abdulmajeed M. Jali: jali@mymail.vcu.edu

23 Dana E. Selley: dana.selley@vcuhealth.org

24 William L. Dewey: william.dewey@vcuhealth.org

25 Hamid I. Akbarali: hamid.akbarali@vcuhealth.org

26 Yan Zhang*: yzhang2@vcu.edu

27 **Corresponding Author**

28 *Telephone: 804-828-0021. Fax: 804-828-7625. E-mail: yzhang2@vcu.edu.

29 **Author Contribution**

30 Y. Zhang conceived and oversaw the project, finalized the manuscript. Y. Zheng, D. A.

31 Williams, C. Zhou and B. Peddibhotla conducted the chemical synthesis. Y. Zheng, S. Obeng

1
2
3 and H. Wang drafted the manuscript together. S. Obeng, A. M. Jali and D. L. Stevens conducted
4 radioligand binding assays and in vivo studies under the supervision of D. E. Selley, W. L.
5 Dewey and H. I. Akbarali. H. Wang finished the docking studies under the supervision of Y.
6 Zhang.
7
8
9
10
11
12
13
14

15 **Funding Sources**

16
17 The authors would like to acknowledge the partial financial support from NIH/NIDA
18 (DA024022 and DA044855)
19
20
21
22
23

24 **Acknowledgements**

25
26 The authors are grateful to NIDA Drug Supply Program for providing the free base of
27 naltrexone. The work is partially supported by NIH/NIDA Grant DA024022 and DA044855.
28 The content is solely the responsibility of the authors and does not necessarily represent the
29 official views of the National Institute on Drug Abuse or the National Institutes of Health.
30
31
32
33
34
35
36
37

38 **Supporting information**

39
40 NMR and IR spectra for 4'-pyridyl carboxylic acids prepared in our lab, HPLC spectra for all
41 newly synthesized NAP derivatives and the shortest distances between atoms on critical amino
42 acid residues and atoms on the ligands of NFP in the MOR, KOR, and DOR were available.
43
44
45
46
47
48

49 **Abbreviations Used**

50
51 opioid-induced constipation (OIC), G-protein-coupled receptor (GPCR), μ opioid receptor
52 (MOR), κ opioid receptor (KOR), δ opioid receptor (DOR), nociception opioid peptide (NOP),
53 inwardly rectifying K^+ (GIRK), voltage-gated Ca^{2+} (VGCC), blood-brain barrier (BBB),
54 Chinese hamster ovary (CHO), compound **1** (NFP), compound **2** (NYP), nuclear magnetic
55
56
57
58
59
60

1
2
3 resonance (NMR), subcutaneous injection (s.c.), National Institute of Drug Abuse (NIDA),
4 Institutional Animal Care and Use Committee (IACUC), naloxone (NLX), confidence level
5
6 (CL), percentage maximum possible effect (%MPE).
7
8
9

10 11 12 **References**

- 13
14
15 (1) Pasternak, G. W. Opioids and their receptors: are we there yet?, *Neuropharmacology* 2014,
16
17 *76 Pt B*, 198-203.
18
19 (2) McNicol, E.; Horowicz-Mehler, N.; Fisk, R. A.; Bennett, K.; Gialeli-Goudas, M.; Chew, P.
20
21 W.; Lau, J.; Carr, D.; American Pain Society. Management of opioid side effects in cancer-
22
23 related and chronic noncancer pain: a systematic review, *J. Pain* **2003**, *4*, 231-256.
24
25 (3) Shang, Y.; Filizola, M. Opioid receptors: Structural and mechanistic insights into
26
27 pharmacology and signaling, *Eur. J. Pharmacol.* **2015**, *763(Pt B)*, 206-213.
28
29 (4) Nutt, D. J. The role of the opioid system in alcohol dependence, *J. Psychopharmacol.* **2014**,
30
31 *28*, 8-22.
32
33 (5) Remesic, M.; Hruba, V. J.; Porreca, F.; Lee, Y. S. Recent advances in the realm of allosteric
34
35 modulators for opioid receptors for future therapeutics. *ACS. Chem. Neurosci.* **2017**, *8*, 1147-
36
37 1158
38
39 (6) Chakrabarti, S.; Prather, P. L.; Yu, L.; Law, P. Y.; Loh, H. H. Expression of the mu-opioid
40
41 receptor in CHO cells: ability of mu-opioid ligands to promote alpha-azidoanilido[³²P]GTP
42
43 labeling of multiple G protein alpha subunits. *J. Neurochem.* **1995**, *64*, 2534-2543.
44
45 (7) Miyake, M.; Christie, M. J.; North, R. A. Single potassium channels opened by opioids in
46
47 rat locus ceruleus neurons. *Proc. Natl. Acad. Sci. USA.* **1989**, *86*, 3419-3422.
48
49 (8) Ortiz-Miranda, S. I.; Dayanithi, G.; Coccia, V.; Custer, E. E.; Alphantery, S.; Mazuc, E.;
50
51 Treisman, S.; Lemos, J. R. mu-Opioid receptor modulates peptide release from rat
52
53 neurohypophysial terminals by inhibiting Ca²⁺ influx. *J. Neuroendocrinol.* **2003**, *15*, 888-894.
54
55
56
57
58
59
60

- 1
2
3 (9) Barchfeld, C. C.; Maassen, Z. F.; Medzihradsky, F. Receptor-related interactions of opiates
4 with PGE-induced adenylate cyclase in brain. *Life Sci.* **1982**, *31*, 1661-1665.
5
6
7 (10) Thorsell, A. The μ -opioid receptor and treatment response to naltrexone. *Alcohol Alcohol.*
8
9 **2013**, *48*, 402-408.
10
11 (11) Herz, A. Multiple opiate receptors and their functional significance. *J. Neural. Transm.*
12
13 *Suppl.* **1983**, *18*, 227-233.
14
15 (12) Sadée, W.; Wang, Z. Agonist induced constitutive receptor activation as a novel regulatory
16
17 mechanism. Mu receptor regulation. *Adv. Exp. Med. Biol.* **1995**, *373*, 85-90.
18
19 (13) Degenhardt, L.; Bucello, C.; Calabria, B.; Nelson, P.; Roberts, A.; Hall, W.; Lynskey, M.;
20
21 Wiessing, L.; GBD illicit drug use writing group.; Mora, M. E.; Clark, N.; Thomas, J.; Briegleb,
22
23 C.; McLaren, J. What data are available on the extent of illicit drug use and dependence
24
25 globally? Results of four systematic reviews. *Drug Alcohol Depend.* **2011**, *117*, 85-101.
26
27 (14) Rehm, J.; Mathers, C.; Popova, S.; Thavorncharoensap, M.; Teerawattananon, Y.; Patra,
28
29 J. Global burden of disease and injury and economic cost attributable to alcohol use and
30
31 alcohol-use disorders. *Lancet* **2009**, *373*, 2223-2233
32
33 (15) Salomon, N.; Perlman, D. C.; Friedmann, P.; Ziluck, V.; Des Jarlais, D. C. Prevalence and
34
35 risk factors for positive tuberculin skin tests among active drug users at a syringe exchange
36
37 program. *Int. J. Tuberc. Lung Dis.* **2000**, *4*, 47-54.
38
39 (16) Nelson, P. K.; Mathers, B. M.; Cowie, B.; Hagan, H.; Des Jarlais, D.; Horyniak, D.;
40
41 Degenhardt, L. Global epidemiology of hepatitis B and hepatitis C in people who inject drugs:
42
43 results of systematic reviews. *Lancet* **2011**, *378*, 571-583.
44
45 (17) Mathers, B. M.; Degenhardt, L.; Phillips, B.; Wiessing, L.; Hickman, M.; Strathdee, S. A.;
46
47 Wodak, A.; Panda, S.; Tyndall, M.; Toufik, A.; Mattick, R. P.; 2007 Reference group to the
48
49 UN on HIV and injecting drug use. Global epidemiology of injecting drug use and HIV among
50
51 people who inject drugs: a systematic review. *Lancet* **2008**, *372*, 1733-1745.
52
53
54
55
56
57
58
59
60

- 1
2
3 (18) Paulozzi, L. J.; Budnitz, D. S.; Xi, Y. Increasing deaths from opioid analgesics in the
4 United States. *Pharmacoepidemiol, Drug Saf.* **2006**, *15*, 618-627.
5
6
7 (19) Degenhardt, L.; Bucello, C.; Mathers, B.; Briegleb, C.; Ali, H.; Hickman, M.; McLaren,
8 J. Mortality among regular or dependent users of heroin and other opioids: a systematic review
9 and meta-analysis of cohort studies. *Addiction* **2011**, *106*, 32-51.
10
11
12 (20) Rudd, R. A.; Seth, P.; David, F.; Scholl, L. Increases in drug and opioid-involved overdose
13 deaths - United States, 2010-2015. *MMWR. Morb. Mortal. Wkly. Rep.* **2016**, *65*, 1445-1452.
14
15
16 (21) Manchikanti, L.; Helm, S. 2nd.; Fellows, B.; Janata, J. W.; Pampati, V.; Grider, J. S.;
17 Boswell, M. V. Opioid epidemic in the United States. *Pain Physician* **2012**, *15*, ES9-38.
18
19
20 (22) Bart, G. Maintenance medication for opiate addiction: the foundation of recovery. *J.*
21 *Addict. Dis.* **2012**, *31*, 207-225.
22
23
24 (23) Stotts, A. L.; Dodrill, C. L.; Kosten, T. R. Opioid dependence treatment: options in
25 pharmacotherapy. *Expert. Opin. Pharmacother.* **2009**, *10*, 1727-1740.
26
27
28 (24) O'Connor, P. G. Methods of detoxification and their role in treating patients with opioid
29 dependence. *J. A. M. A.* **2005**, *294*, 961-963.
30
31
32 (25) Martell, B. A.; Arnsten, J. H.; Krantz, M. J.; Gourevitch, M. N. Impact of methadone
33 treatment on cardiac repolarization and conduction in opioid users. *Am. J. Cardiol.* **2005**, *95*,
34 915-918.
35
36
37 (26) Bart, G. CSAT's QT interval screening in methadone report: outrageous fortune or sea of
38 troubles? *J. Addict. Dis.* **2011**, *30*, 313-317.
39
40
41 (27) Ducharme, S.; Fraser, R.; Gill, K. Update on the clinical use of buprenorphine in opioid-
42 related disorders. *Can. Fam. Physician* **2012**, *588*, 37-41.
43
44
45 (28) Saidak, Z.; Blake-Palmer, K.; Hay, D. L.; Northup, J. K.; Glass, M. Differential activation
46 of G-proteins by mu-opioid receptor agonists. *Br. J. Pharmacol.* **2006**, *147*, 671-680.
47
48
49 (29) Helm, S.; Trescot, A. M.; Colson, J.; Sehgal, N.; Silverman, S. Opioid antagonists, partial
50
51
52
53
54
55
56
57
58
59
60

agonists, and agonists/antagonists: the role of office-based detoxification. *Pain Physician* **2008**, *11*, 225-235.

(30) Pelton, J. T.; Kazmierski, W.; Gulya, K.; Yamamura, H. I.; Hruby, V. J. Design and synthesis of conformationally constrained somatostatin analogues with high potency and specificity for mu opioid receptors. *J. Med. Chem.* **1986**, *29*, 2370-2375.

(31) Hawkins, K. N.; Knapp, R. J.; Lui, G. K.; Gulya, K.; Kazmierski, W.; Wan, Y. P.; Pelton, J. T.; Hruby, V. J.; Yamamura, H. I. [³H]-[H-D-Phe-Cys-Tyr-D-Trp-Orn-Thr-Pen-Thr-NH₂] ([³H]CTOP), a potent and highly selective peptide for mu opioid receptors in rat brain. *J. Pharmacol. Exp. Ther.* **1989**, *248*, 73-80.

(32) Abbruscato, T. J.; Thomas, S. A.; Hruby, V. J.; Davis T. P. Blood-brain barrier permeability and bioavailability of a highly potent and mu-selective opioid receptor antagonist, CTAP: comparison with morphine. *J. Pharmacol. Exp. Ther.* **1997**, *280*, 402-409.

(33) Darke, S.; Hall, W. Heroin overdose: research and evidence-based intervention. *J. Urban Health* **2003**, *80*, 189-200.

(34) White, J. M.; Irvine, R. J. Mechanisms of fatal opioid overdose. *Addiction* **1999**, *94*, 961-972.

(35) Ngo, H. T.; Tait, R. J.; Hulse, G. K. Comparing drug-related hospital morbidity following heroin dependence treatment with methadone maintenance or naltrexone implantation. *Arch. Gen. Psychiatry.* **2008**, *65*, 457-465.

(36) Dhopes, V. P.; Taylor, K. R.; Burke, W. M. Survey of hepatitis B and C in addiction treatment unit. *Am. J. Drug Alcohol Abuse* **2000**, *26*, 703-707.

(37) Hallinan, R.; Byrne, A.; Amin, J.; Dore, G. J. Hepatitis C virus prevalence and outcomes among injecting drug users on opioid replacement therapy. *J. Gastroenterol. Hepatol.* **2005**, *20*, 1082-1086.

(38) van Dorp, E.; Yassen, A.; Dahan, A. Naloxone treatment in opioid addiction: the risks and

benefits. *Expert. Opin. Drug Saf.* **2007**, *6*, 125-132.

(39) Filliol, D.; Ghozland, S.; Chluba, J.; Martin, M.; Matthes, H. W.; Simonin, F.; Befort, K.; Gavériaux-Ruff, C.; Dierich, A.; LeMeur, M.; Valverde, O.; Maldonado, R.; Kieffer, B. L. Mice deficient for delta- and mu opioid receptors exhibit opposing alterations of emotional responses. *Nat. Genet.* **2000**, *25*, 195-200.

(40) Jutkiewicz, E. M. The antidepressant-like effects of delta-opioid receptor agonists. *Mol. Interv.* **2006**, *6*, 162-169.

(41) Wang, X.; Dergacheva, O.; Griffioen, K. J.; Huang, Z. G.; Evans, C.; Gold, A.; Bouairi, E.; Mendelowitz, D. Action of kappa and delta opioid agonists on premotor cardiac vagal neurons in the nucleus ambiguus. *Neurosci.* **2004**, *129*, 235-241.

(42) Lishmanov, A. I.; Lasukova, T. V.; Maslov, L. N.; Platonov, A. A. Role of kappa-opioid receptors in the regulation of cardiac resistance to arrhythmogenic effects of ischemia and reperfusion. *Ross. Fiziol. Zh. Im. I. M. Sechenova.* **2006**, *92*, 1419-1428.

(43) Valtchanova-Matchouganska, A.; Missankov, A.; Ojewole, J. A. Evaluation of the antidysrhythmic effects of delta- and kappa-opioid receptor agonists and antagonists on calcium chloride-, adrenaline- and ischemia/reperfusion-induced arrhythmias in rats. *Methods Find Exp. Clin. Pharmacol.* **2004**, *26*, 31-38.

(44) a). Li, G.; Aschenbach, L. C.; Chen, J.-Y.; Cassidy, M. P.; Stevens, D. L.; Gabra, B. H.; Selley, D. E.; Dewey, W. L.; Westkaemper, R. B.; Zhang, Y. Design, synthesis, and biological evaluation of 6 α - and 6 β -N-heterocyclic substituted naltrexamine derivatives as μ opioid receptor selective antagonists. *J. Med. Chem.* **2009**, *52*, 1416-1427. b). Ward, S. J.; Portoghese, P. S.; Takemori, A. E. Pharmacological profiles of β -funaltrexamine (β -FNA) and β -chlornaltrexamine (β -CNA) on the mouse vas deferens preparation. *Eur. J. Pharmacol.* **1982**, *80*, 377-384.

(45) Schmidhammer, H.; Burkard, W. P.; Eggstein-Aeppli, L.; Smith, C. F. Synthesis and

1
2
3 biological evaluation of 14-alkoxymorphinans. 2. (-)-N-(cyclopropylmethyl)-4,14-
4 dimethoxymorphinan-6-one, a selective mu opioid receptor antagonist. *J. Med. Chem.* **1989**,
5
6 32, 418-421.
7
8

9
10 (46) Spetea, M.; Schüllner, F.; Moisa, R. C.; Berzetei-Gurske, I. P.; Schraml, B.; Dörfler, C.;
11
12 Aceto, M. D.; Harris, L. S.; Coop, A.; Schmidhammer, H. Synthesis and biological evaluation
13
14 of 14-alkoxymorphinans. 21. Novel 4-alkoxy and 14-phenylpropoxy derivatives of the mu
15
16 opioid receptor antagonist cyprodime. *J. Med. Chem.* **2004**, *47*, 3242-3247.
17
18

19 (47) Broadbear, J. H.; Sumpter, T. L.; Burke, T. F.; Husbands, S. M.; Lewis, J. W.; Woods, J.
20
21 H.; Traynor, J. R.; Methocinnamox is a potent, long-lasting, and selective antagonist of
22
23 morphine-mediated antinociception in the mouse: comparison with clocinnamox, beta-
24
25 funaltrexamine, and beta-chlornaltrexamine. *J. Pharmacol. Exp. Ther.* **2000**, *294*, 933-940.
26
27

28 (48) Butelman, E. R.; Yuferov, V.; Kreek, M. J. κ -Opioid receptor/dynorphin system: Genetic
29
30 and pharmacotherapeutic implications for addiction. *Trends Neurosci.* **2012**, *35*, 587-596.
31
32

33 (49) Spanagel, R.; Almeida, O. F.; Bartl, C.; Shippenberg, T. S. Endogenous kappa-opioid
34
35 systems in opiate withdrawal: Role in aversion and accompanying changes in mesolimbic
36
37 dopamine release. *Psychopharmacology* **1994**, *115*, 121-127.
38
39

40 (50) a). Simonin, F.; Valverde, O.; Smadja, C.; Slowe, S.; Kitchen, I.; Dierich, A.; Le Meur,
41
42 M.; Roques, B. P.; Maldonado, R.; Kieffer, B. L. Disruption of the kappa-opioid receptor gene
43
44 in mice enhances sensitivity to chemical visceral pain, impairs pharmacological actions of the
45
46 selective kappa-agonist U-50, 488H and attenuates morphine withdrawal. *E. M. B. O. J.* **1998**,
47
48 *17*, 886-897. b.) De Marco, R.; Bedini, A.; Spampinato, S.; Comellini, L.; Zhao, J.; Artali, R.;
49
50 Gentilucci, L. Constraining endomorphin-1 by β,α -hybrid dipeptide/heterocycle scaffolds:
51
52 identification of a novel κ -opioid receptor selective partial agonist. *J. Med. Chem.* **2018**, *61*,
53
54 5751-5757.
55
56
57

58 (51) Pelotte, A. L.; Smith, R. M.; Ayestas, M.; Dersch, C. M.; Bilsky, E. J.; Rothman, R. B.;
59
60

1
2
3 Deveau, A. M. Design, synthesis, and characterization of 6 β -naltrexol analogs, and their
4 selectivity for in vitro opioid receptor subtypes. *Bioorg. Med. Chem. Lett.* **2009**, *19*, 2811-2814.

5
6
7 (52) Ward, S. J.; Portoghese, P. S.; Takemori, A. E. Pharmacological characterization in vivo
8 of the novel opiate, beta-funaltrexamine. *J. Pharmacol. Exp. Ther.* **1982**, *220*, 494-498.

9
10
11 (53) Yekkirala, A. S.; Lunzer, M. M.; McCurdy, C. R.; Powers, M. D.; Kalyuzhny, A. E.;
12 Roerig, S. C.; Portoghese, P. S. N-naphthoyl-beta-naltrexamine (NNTA), a highly selective
13 and potent activator of μ /kappa-opioid heteromers. *Proc. Natl. Acad. Sci. USA.* **2011**, *108*,
14 5098-5103.

15
16
17 (54) Yuan, Y.; Li, G.; He, H.-J; Stevens, D. L.; Kozak, P.; Scoggins, K. L.; Mitra, P.; Gerk, P.
18 M.; Selley, D. E.; Dewey, W. L.; Zhang, Y. Characterization of 6 α - and 6 β -N-heterocyclic
19 substituted naltrexamine derivatives as novel leads to development of mu opioid receptor
20 selective antagonists. *ACS Chem. Neurosci.* **2011**, *2*, 346-351.

21
22 (55) a). Mitra, P.; Venitz, J.; Yuan, Y.; Zhang, Y.; Gerk, P. M. Preclinical disposition (in vitro)
23 of novel μ -opioid receptor selective antagonists. *Drug Metab. Dispos.* **2011**, *39*, 1589-1596.

24
25 b.) Hernández-Delgadillo, G. P.; Cruz, S. L. Endogenous opioids are involved in morphine and
26 dipyrone analgesic potentiation in the tail flick test in rats. *Eur. J. Pharmacol.* **2006**, *546*, 54-
27 59.

28
29 (56) Yuan, Y.; Stevens, D. L.; Braithwaite, A.; Scoggins, K. L.; Bilsky, E.; Akbarali, H. I.;
30 Dewey, W. L.; Zhang, Y. 6 β -N-Heterocyclic substituted naltrexamine derivative as potential
31 lead to develop peripheral mu opioid receptor selective antagonists. *Bioorg. Med. Chem. Lett.*
32 **2012**, *22*, 4731-4734.

33
34 (57) a). Yuan, Y.; Elbegdorj, O.; Chen, J.; Akubathini, S. K.; Zhang, F.; Stevens, D. L.;
35 Beletskaya, I. O.; Scoggins, K. L.; Zhang, Z.; Gerk, P. M.; Selley, D. E.; Akbarali, H. I.; Dewey,
36 W. L.; Zhang, Y. Design, synthesis, and biological evaluation of 17-cyclopropylmethyl-3,14 β -
37 dihydroxy-4,5 α -epoxy-6 β -[(4'-pyridyl)carboxamido]morphinan derivatives as peripheral
38
39
40
41
42
43
44
45
46
47
48
49
50
51
52
53
54
55
56
57
58
59
60

1
2
3 selective μ opioid receptor Agents. *J. Med. Chem.* **2012**, *55*, 10118-10129. b). Yakhontov, L.
4 Y.; Lapan, E. I.; Rubtsov, M. V. The synthesis of isomeric 4- and 6-ethoxy-3-ethylpyridines.
5
6 *Chem. Heterocyclic Com.* **1967**, *3*, 829-831. c). Xin, B. W. Phosphine-free cross-coupling
7
8 reaction of halopyridines with arylboronic acids in an ionic liquid: water mixture. *J. Chem.*
9
10 *Res.* **2008**, *2008*, 412-415. d). Okawa, T.; Aramaki, Y.; Yamamoto, M.; Kobayashi, T.;
11
12 Fukumoto, S.; Toyoda, Y.; Henta, T.; Hata, A.; Ikeda, S.; Kaneko, M.; Hoffman, I. D.; Sang,
13
14 B. C.; Zou, H.; Kawamoto, T. Design, synthesis, and evaluation of the highly selective and
15
16 potent G-protein-coupled receptor kinase 2 (GRK2) inhibitor for the potential treatment of
17
18 heart failure. *J. Med. Chem.* **2017**, *60*, 6942-6990.
19
20
21

22
23 (58) Wang, H.; Zaidi, S. A.; Zhang, Y. Binding mode analyses of NAP derivatives as mu opioid
24
25 receptor selective ligands through docking studies and molecular dynamics simulation. *Bioorg.*
26
27 *Med. Chem.* **2017**, *25*, 2463-2471.
28
29

30
31 (59) Hagmann, W. K. The many roles for fluorine in medicinal chemistry. *J. Med. Chem.* **2008**,
32
33 *51*, 4359-4369.
34

35
36 (60) Mahar Doan, K. M.; Humphreys, J. E.; Webster, L. O.; Wring, S. A.; Shampine, L. J.;
37
38 Serabjit-Singh, C. J.; Adkison, K. K.; Polli, J. W. Passive permeability and P-glycoprotein-
39
40 mediated efflux differentiate central nervous system (CNS) and non-CNS marketed drugs. *J.*
41
42 *Pharmacol. Exp. Ther.* **2002**, *303*, 1029-1037.
43
44

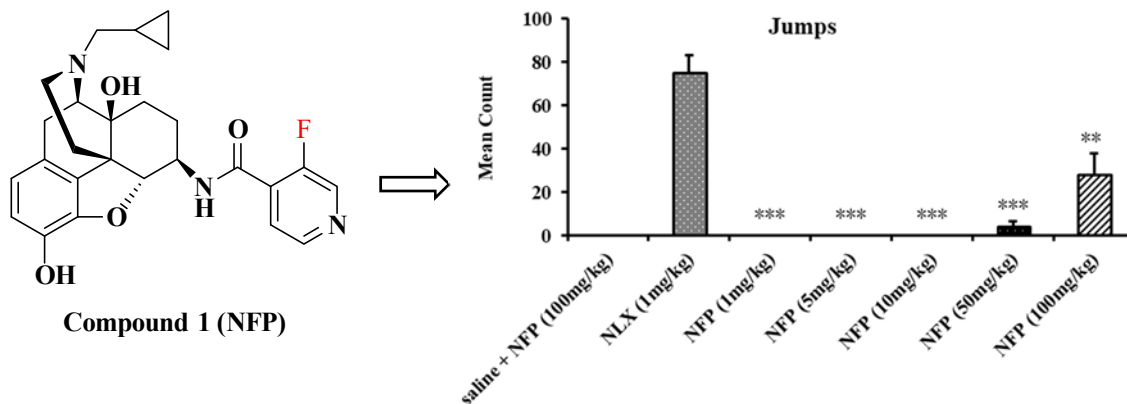
45
46 (61) Christie, M. J. Cellular neuroadaptations to chronic opioids: tolerance, withdrawal and
47
48 addiction. *Br. J. Pharmacol.* **2008**, *154*, 384-396.
49

50
51 (62) Fleming, F. F.; Yao, L.; Ravikumar, P. C.; Funk, L.; Shook, B. C. Nitrile-containing
52
53 pharmaceuticals: efficacious roles of the nitrile pharmacophore. *J. Med. Chem.* **2010**, *53*, 7902-
54
55 7917.
56

57
58 (63) Brack, A.; Bottiger, B. W.; Schafer, M.; New insights in postoperative pain therapy.
59
60 *Anesthesiol Intensivmed Schmerzther* **2004**, *39*, 157-164

- 1
2
3 (64) Manglik, A.; Kruse, A. C.; Kobilka, T. S.; Thian, F. S.; Mathiesen, J. M.; Sunahara, R.
4 K.; Pardo, L.; Weis, W. I.; Kobilka, B. K.; Granier, S. Crystal structure of the micro-opioid
5 receptor bound to a morphinan antagonist. *Nature* **2012**, *485*, 321-326.
6
7
8
9
10 (65) Wu, H.; Wacker, D.; Mileni, M.; Katritch, V.; Han, G. W.; Vardy, E.; Liu, W.; Thompson,
11 A. A.; Huang, X. P.; Carroll, F. I.; Mascarella, S. W.; Westkaemper, R. B.; Mosier, P. D.; Roth,
12 B. L.; Cherezov, V.; Stevens, R. C. Structure of the human κ -opioid receptor in complex with
13 JD1c. *Nature* **2012**, *485*, 327-332.
14
15
16
17
18 (66) Granier, S.; Manglik, A.; Kruse, A. C.; Kobilka, T. S.; Thian, F. S.; Weis, W. I.; Kobilka,
19 B. K. Structure of the δ -opioid receptor bound to naltrindole. *Nature* **2012**, *485*, 400-404.
20
21
22
23 (67) Jones, G.; Willett, P.; Glen, R. C.; Leach, A. R.; Taylor, R. Development and validation
24 of a genetic algorithm for flexible docking. *J. Mol. Biol.* **1997**, *267*, 727-748.
25
26
27
28 (68) Jones, G.; Willett, P.; Glen, R. C. Molecular recognition of receptor sites using a genetic
29 algorithm with a description of desolvation. *J. Mol. Biol.* **1995**, *245*, 43-53.
30
31
32
33 (69) Ballesteros, J. A.; Weinstein, H. Integrated methods for the construction of three-
34 dimensional models and computational probing of structure-function relations in G protein-
35 coupled receptors. *Methods in Neuroscience* **1995**, *25*, 366-428.
36
37
38
39 (70) Clark, M.; Cramer, R. D.; Van Opdenbosch, N. Validation of the general purpose tripos
40 5.2 force field. *J. Comput. Chem.* **1989**, *10*, 982-1012.
41
42
43
44
45
46
47
48
49
50
51
52
53
54
55
56
57
58
59
60

Table of Contents Graphic



NFP induced significantly less withdrawal symptoms compared to naloxone in the morphine-pelleted mice.